UNIL | Université de Lausanne
Faculté de biologie
et de médecine

# Detection of Ectodysplasin A and phenotypic characterization of its deficiency

December 9, 2014

Master Thesis in Medicine N° 244

Heidi Sarrasin

Director
Dr. Pascal Schneider
Department of Biochemistry, UNIL

Expert
Dr. Olivier Gaide
Department of Dermatology, CHUV

# Contents


**1 Abstract** **4**

**2 Introduction** **5**
2.1 Hypohidrotic ectodermal dysplasia . . . 5
2.2 Phenotype of HED . . . 5
2.3 Diagnosis . . . 6
2.4 Management . . . 7
2.5 Curative therapy . . . 7
2.6 The TNF superfamily . . . 7
2.7 EDA and EDAR . . . 8
2.8 Activation of the NF-$\kappa$B pathway . . . 9
2.9 Mouse models for hypohidrotic ectodermal displasia . . . 9
2.10 Ectodermal appendages organogenesis . . . 10
2.11 Anatomical and histolgical description of mouse nasal cavity . . . 11
2.12 Nasal secretions function . . . 12

**3 Aims** **12**

**4 Material et method** **12**
4.1 ELISA . . . 12
4.2 Histology . . . 16

**5 Results** **17**
5.1 ELISA . . . 17
5.1.1 Characterization of anti-EDA antibodies . . . 17
5.1.2 EctoD2 and EctoD3 prevent the interaction of EDA1 with EDAR . . . 17
5.1.3 Sensitive detection of Fc-EDA by sandwich ELISA . . . 19
5.1.4 Detection of endogenous EDA . . . 20
5.2 Histology . . . 23
5.2.1 Localisation of the nasal, lacrimal, and ceruminous glands . . . 23
5.2.2 Nasal, lacrimal, and ceruminous glands in the *EDA*-deficient Tabby mouse . . . 27
5.2.3 5.2.3. Nasal, lacrimal, and ceruminous glands response in mice treated with an EDAR agonist . . . 27

**6 Discussion** **31**

**7 Acknowledgment** **33**

**8 Bibliography** **33**

# 1 Abstract

Ectodysplasin A (EDA), a trimeric ligand of the TNF super-family, is implicated in the embryonic development of ectodermal appendages such as hairs, teeth, sweat glands and other types of glands. Inactivating mutations in the *EDA* gene located on the X-chromosome cause X-linked hypohidrotic ectodermal dysplasia (XLHED), a disease characterized by the absence or malformation of structures derived from the ectoderm. Although EDA is synthetized as a membrane-bound protein, it can be cleaved and released in a soluble form, but it is not known whether soluble EDA can be detected.
Stimulation of EDA receptor (EDAR) during development in *EDA*-deficient animals can correct the phenotype of EDA deficiency. It is however unknown whether EDAR stimulation in adult mice might affect exocrine glands in the nasal cavity, eyes and ears.

Objectives:

1. One aim was to develop a method for the detection of endogenous EDA.
2. A second aim was to localize exocrine glands in the nasal cavity, eyes and ears of wild-type and *EDA*-deficient adult mice and to evaluate the impact on these glands of a chronic, post-developmental stimulation of EDAR.

Methods:

1. A sandwich ELISA was used to detect EDA in sera of different species (human, foetal calf, mouse). Serum pre-depletions were performed to address the nature of the signal detected. For this purpose, EDA-binding reagents distinct from the pair of anti-EDA antibodies used in the sandwich ELISA were used.
2. Adult *EDA*-deficient mice were treated for 12 weeks by intraperitoneal injections of an EDAR agonist. Localization, size and morphology of exocrine glands in the nasal cavity, eye and ear were monitored in histology sections.

Results: Endogenous levels of circulating EDA were detected in human and bovine, but not in mouse sera. Pre-depletion on recombinant EDAR could remove about half of the signal, confirming the presence of receptor-binding competent EDA in the serum.
A variety of exocrine glands were localized by histology in the nasal cavity, eyes and ears of WT and *EDA*-deficient mice. Differences were noticed across genotypes, but no obvious effect of treatment on the presence or morphology of these glands was detected.

Importance: A clinical trial for the orphan disease XLHED based on neonatal administration of an EDAR agonist is currently on-going. In this context, the detection of endogenous EDA in serum is relevant. Indeed, this could be exploited to establish a diagnostic screen for EDA-deficiency.

# 2 Introduction

Ectodermal dysplasias (ED) form a heterogeneous group of more than 150 clinically distinct congenital diseases characterized by abnormal development of ectodermal structures and skin appendages (1,2). Initiation, formation and differentiation of many ectodermal appendages are under control of Ectodysplasin A (EDA), a ligand of the tumor necrosis factor (TNF) superfamily. Three proteins are specific to the EDA signalling pathway: the ligand EDA1, its receptor EDAR, and a cytosolic adaptor EDARADD (EDAR-associated death domain). Engagement of the EDA pathway activates the transcription factor NF-$\kappa$B (3,4). Mutations in genes of this pathway cause hypohidrotic ectodermal dysplasia (HED) the most common form of ED. The incidence of ED is estimated at 1:100,000 live births.(5)

## 2.1 Hypohidrotic ectodermal dysplasia

Hypohidrotic ectodermal dysplasia (HED) also named the Christ-Siemens-Touraine syndrome (5) is a rare genodermatosis characterized by a triad of symptoms: missing or sparse hair (atrichosis or hypotrichosis), missing or dysmorphic teeth (anodontia or hypodontia), and absence or reduced sweating (anhydrosis or hypohydrosis) (1,6). The incidence of HED is also estimated at 1:100,000 births (7).

In human, three modes of inheritance of HED have been described: X-linked, autosomal recessive and autosomal dominant (3). X-linked HED (XLHED), the most common form of HED (7), is caused by mutations in the EDA gene on chromosome Xq12-q13.1 (MIM #305100). Mutations in the EDAR gene located on chromosome 2q11-q13 (MIM #604095) or on the EDARADD gene located on chromosome 1q42-q43 (MIM #606603) can generate both autosomal recessive or dominant forms, depending on the nature of the mutation (4,6). Reported mutations include large deletions, insertions, small in-frame deletions, and missense and nonsense mutations (1). Mutations in either of these three genes produce similar phenotypes characterized by absence or malformation of teeth, hair, sweat glands and other glands (1,2,4).

Males with XLHED, and males and females with the autosomal recessive form have the classical form of HED, as described below. Milder form of HED can be found in female carriers of XLHED and in males and females with the autosomal dominant form (6).

## 2.2 Phenotype of HED

Hair, teeth, sweat glands and other glands are typically missing or malformed in HED and are responsible for the main clinical features of the disease. The following paragraphs describe the HED phenotype (Fig. 1).

Body hair is sparse. Patients usually also present thin, light and slow-growing scalp hairs. Secondary sexual hair however develop relatively normally (6).

Regarding dentition, an average of nine permanent teeth develop in individual with classical HED (6). Teeth are usually described as missing or peg-shaped and erupt later than expected. This leads to difficulties with mastication, growth retardation, poor appearance and speech difficulties (5,8,9).

The most important feature of HED is life-threatening hyperthermia. Indeed, the absent or deficient sweating prevents patients from responding correctly to an increase of their body temperature, for example in case of high fever (3). Risk of febrile seizure exists even if psychomotor development is usually within normal limits (6,8). Unrecognized syndrome can lead to 30% mortality rate during the first two years of life (1).

Salivary, sebaceous, nasal, and lacrimal glands are some of the other glands affected in HED. Indeed, patients produce insufficient saliva that causes oral dryness and they have difficulties chewing and swallowing specific aliments. In addition, their voice can change. Regarding ears, the most common findings are otitis media, hearing loss and cerumen impactions that can lead to auditory canal stenosis. Because of inadequate nasal secretions, patients describe obstruction, dryness, crusting, and sinusitis. People suffering from HED often have dry eyes symptoms and conjunctivitis due to abnormal Meibomian glands (5,8–10).

In addition, patients present an increased risk of chest infections probably due to deficient mucus production. They also present higher prevalence of atopic disease like eczema and wheezing typical of asthma (8).

Patient with HED present typical facial features with depressed nasal bridge or saddle nose deformity and periorbital hyperpigmentation (5,8,9).

Figure 1: Phenotypic features of hypohidrotic ectodermal dysplasia (1).

### 2.3 Diagnosis

HED can be diagnosed by the presence of the three cardinal features: hypotrichosis, hypodontia, hypohydrosis.

Hypothrichosis and hypodontia are evaluated by clinical observation of missing hair and teeth respectively. Moreover, to determine the extent of hypodontia dental radiograph can be helpful. To evaluate the developing dentition, a palpation of dental alveolus permits to establish if developing tooth buds are present.

Concerning hypohydrosis, sweat glands function can be assessed by sweat tests using iodine solution. Furthermore, the number and distribution of sweat pores can be determined using an impression material.

Even if it is possible to diagnose HED by clinical observation, genetic testing is useful to confirm or establish a diagnosis, to detect carriers and to establish prenatal diagnosis. A genetic counselling including a review of family history and examination of at-risk relatives allows determining the mode of inheritance and helps provide the family with an early support (6).

## 2.4 Management

Management of HED targets the three cardinal features. Patients benefit from wigs, special care formulas and techniques to manage sparse hairs.

Regarding dental treatments, they can vary from simple restoration to dentures, and they must begin at an early age.

To reduce the risk of hyperthermia, patients must have access to adequate supply of water and a cool environment. Good care should be taken to prevent heat exposure and the risk of febrile seizure.

For the other features of HED, there are specific managements. Because of hypo-salivation, patient benefit of therapeutics maintaining oral lubrication and caries control, that means saliva substitute and fluoride exposure. Children with chewing and swallowing problems may benefit from dietary counselling (6,10,11).

## 2.5 Curative therapy

Besides supportive therapies, there is nowadays no curative treatment of HED (12), although results obtained in *Eda*-deficient mice and dogs with an experimental EDA1 replacement therapy provides good hope for an effective and targeted therapy.

Indeed, if a recombinant Fc-EDA1 protein is provided during the embryonic and postnatal periods in Eda-deficient mice, most of the phenotypic characteristics of XLHED can be corrected. These data also showed that Fc-EDA1 was required to induce ectodermal appendages development, but was not require for long term maintenance of these structures (13).

The canine model of XLHED, which is closer to the human disease, was also used to assess the effect of the EDA1 replacement therapy. XLHED in dogs is clinically quite similar to human. Indeed, dogs unlike mice have both deciduous and permanent teeth. Postnatal intravenous injections of recombinant EDA permitted the normalisation of teeth and also improved other important feature of the XLHED (14). Because diagnosis of XLHED is often established only after birth, the positive results of postnatal treatment in dogs suggest that it may also work post-natally in human (12–14).

## 2.6 The TNF superfamily

The tumour necrosis factor (TNF) superfamily includes 19 ligands (encoded by 18 genes) which fulfil their functions through 29 receptors (15). Functions regulated by the TNF superfamily are wide: immune and inflammatory response, haematopoiesis, morphogenesis, but also anti-tumour surveillance, transplant rejection, septic shock and viral replication (3,16). After binding to their receptors, ligands can induce responses as diverse as cell proliferation, differentiation, survival or apoptosis (15,16). Ligands and receptors of the TNF superfamily have typical conserved structures and a conserved mode of activation (15).

TNF ligands are type II transmembrane proteins (*i.e.* with an intracellular N-terminus) that share a structurally conserved extracellular C-terminal domain called the TNF homology domain (THD). The THD folds as a homo-trimeric structure containing the receptor binding sites. Most transmembrane TNF family ligands can be released in soluble forms by proteolysis (15).

TNF receptors are type I transmembrane proteins (*i.e.* with an extracellular N-terminus) characterized by the presence of one to four cysteine-rich domains in their extracellular portion. The TNF homology domain of the TNF ligand binds these cysteine-rich domains (15). A pre-ligand binding domain has been identified in the N-terminal portion of the several receptors, including TNFR1. It permits self-association of receptors before ligand binding (15). Crystallographic studies have shown repeatedly that trimeric ligands interact with three monomeric receptors, forming a hexameric structure that probably represents the basal unit for signalling (15).

After binding to their respective ligands, most TNF receptors recruit TNFR-associated factors (TRAFs), which are intracellular adaptor proteins involved in the activation of the NF-$\kappa$B transcription factor (1,15).

In the TNF superfamily, APRIL, BAFF and TWEAK are the closest homologues of EDA, even if only the later contains a collagen domain. The overall structure of EDA also resembles that of C1q proteins, which have a globular trimeric C-terminal domain homologous to the THD and a collagenous domain which mediate the multimerization of the trimers (1,17).

## 2.7 EDA and EDAR

The EDA transcript is subject to alternative splicing of the 12 exons producing numerous EDA transcript isoforms (1,7,18). EDA1 (391 amino acids) and EDA2 (389 amino acids), the longest splice variants, are the only variants containing the THD and therefore able to activate TNFR family receptors. These two isoforms only differ by two amino acids in their TNF homology domain, which is however sufficient to switch receptor-binding specificity. Indeed, EDA1 binds EDAR and EDA2 binds the X-linked Ectodysplasin-A2 receptor (XEDAR) (7,18,19).

Both EDA1 and EDA2 are produced as trimeric type II transmembrane proteins with a small N-terminal intracellular domain and a larger C-terminal extracellular domain (1,17). The C-terminal extracellular region of EDA contains four functionally important domain: i) a furin cleavage site that permits, upon proteolytic processing, to release a soluble protein; ii) a proteoglycan binding domain; iii) a collagen domain with 19 Gly-X-Y repeats required to multimerize soluble EDA trimers and iv) a C-terminal TNF homology domain (THD) conferring receptor binding ability (17,20). In brief, proteolytic processing, oligomerisation, and specific receptor binding ability of EDA are essential for its action in vivo (17), while the role of the interaction with proteoglycans remains to be determined (20).

EDAR is a type I transmembrane protein (448 amino acids) composed by an extracellular N-terminal domain containing the cysteine-rich domains, a single transmembrane domain and a long C-terminal intracellular portion that contains a death domain (DD). On the other hand, XEDAR is a type III transmembrane protein, existing as two splice variants of 297 or 318 amino acids, with no N-terminal signal peptide (1,21).

As described above, HED has been associated with mutations in EDA, EDAR, and EDARADD (4,7). Mutations in EDA1 causing XLHED are the most common and affect the three functionally important domains of the protein, namely the he furin recognition site, the collagen domain and the TNF homology domain (1,17). A wide spectrum of genetic defect have been describe in the *EDA* gene (1,4). For *EDAR* and *EDARADD*, fewer mutations have been

identified (1,7).

## 2.8 Activation of the NF-$\kappa$B pathway

NF-$\kappa$B transcription factors regulates expression of genes involved in immune and inflammatory responses, in stress responses, in inflammation and cell adhesion, but also in skin appendages development (3). There are two main mechanisms to activate NF-$\kappa$B: the canonical and the alternative NF-$\kappa$B signalling pathways (22).

The canonical signalling pathway involves the release of the NF-$\kappa$B dimer RelA/p50 via an inducible degradation of the NF-$\kappa$B inhibitor, I$\kappa$B$\alpha$, by the I$\kappa$B kinase (IKK) complex. This process permits a rapid and transient nuclear translocation of NF-$\kappa$B (16,18,21,22).

The alternative signalling pathway regulates important functions like lymphoid organogenesis, B-cell survival and maturation, dendritic cell activation, and bone metabolism. Instead of degradation of I$\kappa$B$\alpha$ to liberate the p50-containing NF-$\kappa$B, the alternative pathway requires p100 processing - p100 is a protein containing an inhibitory domain analogous to I$\kappa$B$\alpha$, and a p52 DNA-binding domain analogous to p50 - to generate p52 and permits the persistent nuclear translocation of a RelB/p52 complex (22).

The activation of the canonical NF-$\kappa$B signalling pathway by EDAR depends on EDA1 and EDARADD (18). After being released from the membrane by proteolytic processing, oligomeric EDA1 trimers bind EDAR (18,19). Once activated, EDAR recruits the adaptor EDARADD that itself binds and activate TRAF (TNFR-associated factor) molecules (1,3).

EDARADD (208 amino acids) consists of an N-terminal TRAF-binding consensus sequence and a C-terminal death domain (1). *In vivo* studies have shown that EDARADD mostly binds to TRAF6. Other evidences have shown that TAB2 (TAK1 binding protein2) bridges TRAF6 to TAK1 (TGF$\beta$-activated kinase 1) (18) with subsequent IKK (I$\kappa$B kinase) complex stimulation, which is an important point in the activation of the NF-$\kappa$B pathway (1,18,21).

NF-$\kappa$B dimers (*e.g.* RelA and p50) are kept in an inactive form in the cytoplasm through I$\kappa$B inhibitory proteins such as I$\kappa$B$\alpha$. I$\kappa$B$\alpha$ in the NF-$\kappa$B complex is phosphorylated by the activated IKK complex, which is composed of two kinase subunits IKK$\alpha$ and IKK$\beta$ (also known as IKK1 and 2) and a regulatory component called NEMO (NF-$\kappa$B essential modulator, also named IKK$\gamma$). Subsequent ubiquitination and degradation by the proteasome machinery of I$\kappa$B proteins permits NF-$\kappa$B to enter the nucleus and activate transcription (3,18,21).

## 2.9 Mouse models for hypohidrotic ectodermal displasia

Four mice mutants (Tabby, Downless, Sleek, Crinkled) have already been described in the 50s with phenotypic resemblances to HED. The Tabby gene located on the X-chromosome has been identified to a region that is syntenic with the EDA human gene suggesting the equivalence of the Tabby syndrome and XLHED. This was confirmed by the cloning of the Tabby gene (23,24).

A recessive mutation in EDAR is found in Downless and a dominant one in Sleek mice. Finally, Crinkled mice carry a mutation in EDARADD (1,18,24).

All three mutations produce comparable phenotypes. Indeed mice have missing and abnormally- shaped teeth, hair defects, and anomalies of several glands (1). Mice pheno-

type has been mainly investigated in the Tabby mouse. Tabby mice have small teeth with few cusps and, with a variable penetrance, sometimes miss incisors and third molar (1). Normal mouse coat is composed of four types of hairs: primary guard hairs, and secondary awl, auchene, and zigzag hairs. Tabby mice have localized alopecia in the retro-auricular region, no hair on the tail, and absent guard and zigzag hairs (1,13). With regard to glands, sweat glands that are located exclusively in footpads and fingers in mice are totally absent. Other glands like lacrimal, Meibomian and salivary glands are either absent or reduced in size (1).

### 2.10 Ectodermal appendages organogenesis

Hair, teeth, sweat glands and other glands are derived from the ectoderm. In HED, these are affected and very different in shape and function. Despite their diversity, ectodermal appendage share common characteristics in development (25).

Ectodermal appendages organogenesis makes use of proliferation, differentiation and cell death and is generally divided into three phases: initiation, morphogenesis, and differentiation (18). Even if initiation occurs during the embryonic period, morphogenesis does continue post-natally (25). Initiation of ectodermal appendages depends on the interaction between the epithelial (ectodermal) layer and the underlying mesenchymal (mesodermal or neural crest) layer (1,18,25). Epithelial-mesenchymal crosstalk is mediated by soluble signalling factors of the FGF (Fibroblast growth factors), BMP (Bone morphogenetic proteins), TGF$\beta$ (transforming growth factor $\beta$ ), Wnt and Hedghogs families. Moreover, EDA is an important early signal for ectodermal organogenesis (1,18,25).

An early stage of ectodermal appendages development consists in formation of placodes, *i.e.* regularly spaced thickening of the epithelial layer, initiated by a "fist dermal signal" from the mesenchyme. Because placodes express many of the above-cited signalling molecules, they are also called embryonic "signalling centres". Then, an "epithelial signal" from the placode causes the condensation of the underlying mesenchymal cells to form a dermal condensate. In response to a "secondary dermal signal" from the dermal condensate, placodal cells proliferate, invade the mesenchyme, and surround the dermal condensate which is called the papilla. Following steps consist in organ-specific epithelium growth and folding (1,18,25,26). In glands, the epithelium develops by several branching. In hair and teeth, the dermal or dental papilla, respectively, get surrounded by an epithelial bud which grows and invaginates (1,25).

The canonical Wnt and BMP pathways are believed to provide the first dermal signal, which promotes appendage formation. Shh was suggested as the secondary epithelial signal for appendage progression and papilla formation (27).

The first dermal signal regulates molecules that either promote or repress placode formation. Proper ectodermal appendage organogenesis depends on strictly regulated interactions between placodal fate promoters and repressors. The contribution of promoters is higher at placodal sites, whereas that of inhibitors is higher at interplacodal sites. Wnts and FGFs are placode promoters, whereas BMPs, in particular BMP2 and BMP4, and TGF$\beta$ inhibit placodal fate. BMPs mediate lateral inhibition (18,25).

EDA is an early and necessary signal for placode formation, indeed, in the absence of EDA signalling, primary hair placodes do not form (18). Spatiotemporal restricted intervals of EDA signalling are needed for proper determination and development of various skin appendages

(27). The EDA pathway lies downstream of the first dermal signal. EDA up-regulates the expression of BMP inhibitors to restrict BMP signalling in the placode during primary hair placode formation. EDA also regulate proliferation and ingrowth of the hair follicle through Shh expression (26,28).

Interestingly, hair growth cycle, composed by anagen, catagen and telogen phases also require cross-talk between ectoderm and mesoderm and analysis suggest that hair follicle morphogenesis mechanisms are reused post-natally (26).

### 2.11 Anatomical and histolgical description of mouse nasal cavity

Mice nose is composed by several anatomical important structures (Fig. 2): the nasal duct, the nasal septum, the inferior maxillary turbinelle, the superior maxillary turbinelle, the true maxillary sinus, three or four ethmoid turbinelle, the anterior ethmoid sinus, the posterior ethmoid sinus, the vomeronasal (Jacobson's) organ, and the nasopharynx (29).

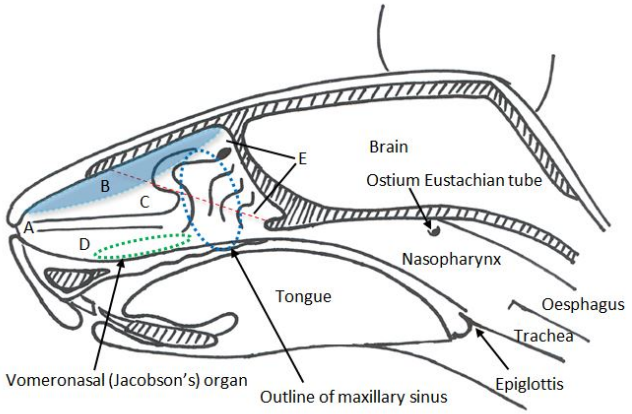


Figure 2: Longitudinal section through the head showing the nasal duct (A), the resected nasal septum (B), the superior maxillary turbinelle (C), the inferior maxillary turbinelle (D) and the ethmoid turbinelles (E). Position of the maxillary sinus is shown in blue, and the location of the vomeronasal (Jacobson's) organ is shown in green. The red line represents the boundary between the respiratory and the olfactory epitheliums.

On an histological perspective, two different epitheliums are present in the nose besides the cutaneous squamous epithelium of the vestibule: the respiratory and the olfactory epitheliums (30,31).

The respiratory pseudo-stratified and ciliated epithelium, containing Goblet cells, covers the anterior and lower part of the nasal cavity. This epithelium also contains intra-epithelial glands. The lamina propria is composed by dense fibrous connective tissue and contains serous and mucous glands and a dense venous plexus (30,32,33). Respiratory epithelium also covers sinuses, with its height diminished and the number of glands and venous plexus decreased (30). The respiratory region warms up and humidifies the breathed air (30).

The olfactory high pseudo-stratified columnar ciliated epithelium covers the superior and posterior part of the nasal cavity. It is composed by olfactory cells, support cells and basal cells. The olfactory glands, also called Bowman glands, are located in the lamina propria

(30,32,33). The olfactory region, as its name suggests, performs the sense of smell.

Most glands contained in the nasal epitheliums are exocrine glands. This type of glands is classified according to structure, and nature of secretion (mucous, serous or mixed). Usually, mucous cells are pale, well delimited and with their nuclei in basal location. On the other hand, serous cells are less well delimited and with spherical central nuclei (33) .

### 2.12 Nasal secretions function

Secretions of mucous cells form a layer at the surface of the nasal epitheliums called mucous. This layer undergoes a constant flow by the ciliary function of the epithelial cells, and thereby is exchanged several times per hour. The mucous protects the nasal mucosa from the environment, by entrapping foreign particles and removing them from the nose (30).

The serous secretion contains protective substances, which can activate immune mechanisms (25).

In the olfactory region, secretions dissolve the olfactory molecules to promote the sense of smell. It also permits to clean the olfactory receptors from the olfactory molecules(30).

## 3 Aims

Mutations on the *EDA* gene cause XLHED disease characterized by abnormal or absent hair, teeth, and sweat glands and other glands. The important aims of this master thesis were:

1. To characterize a pair of antibodies by ELISA assays to detect endogenous EDA e.g. in serum.
2. To localise exocrine nasal glands, lacrimal glands and ceruminous glands of wild-type and *EDA*-deficient adult mice and to evaluate the effect of an agonist treatment on these glands.

## 4 Material et method

### 4.1 ELISA

Antibodies. recombinant proteins and sera

All antibodies and proteins used were available in the laboratory. These included mouse monoclonal IgG1 anti-EDA antibodies, Renzo2 (#1211-08; #1006-30), EctoD1 (#1208-10), EctoD2 (#1208-10), and EctoD3 (#1301-31) (35). Mouse mAb anti-hAPRIL Aprily2 (#1205-04). Fc-EDA1 (APO200, #0701) and Fc-EDA1 (EDI200, #11-0015) were kindly provided by Edimer Pharmaceuticals. Fc-APRIL-2826 (#1303-13). EDAR-Fc-930 (#1106-30; #1004-01). OptiMEM Flag-EDA1-548 at $\tilde{2}$ $\mu$g/ml (#1101-03). EctoD3-biot (#1209-05). Fc-EDA2-1235 (#211-11; #403-25). OptiMEM Flag-EDA2-508 (#811-06). Fc-EDA2-1235 (#211-11; #403-25). OptiMEM Fc-EDA2-1235 (#908-18). Fc-FasL-1117 (#505-23). BCMA-Fc-739 (#712-07). XEDAR-Fc Alexis (#522-049-C050). XEDAR-Fc-1060 (#1011-11). Human serum (Pascal's, #1304-04), FCS (#1309-24), WT (#1304-05) and Tabby (#1304-05) mouse sera.

SDS-PAGE and Coomassie blue staining of antibodies

10 $\mu$g of different antibodies in 20 $\mu$l of PBS were mixed with 10 $\mu$l of 3x concentrated SDS-PAGE sample buffer + dithiothreitol, heated for 5 min at 95°C and size-separated by electrophoresis for 45 min at 200 V in 12% acrylamide SDS-PAGE gels. Gels were stained for 30 minutes an acidic Coomassie blue solution and destained as required in destain solution.

Test anti-EDA antibodies by Western Blot

200 ng of Fc-EDA1-APO200 and Fc-APRIL-2826 were heated for exactly 3 min at 70°C in reducing SDS-PAGE sample buffer. Proteins were resolved on a 12% agarose SDS-PAGE at 200 V for 45 min in running buffer and transferred onto a nitrocellulose membrane at 100 V for 1 h in blotting buffer. The membrane was stained with Ponceau red and then blocked for 1 h at room temperature in block buffer. The membrane was revealed with Renzo2, EctoD1, EctoD2, EctoD3 or Aprily2 at 1 $\mu$g/ml in PBS milk, or HRP-coupled anti-Fc antibody at 1:5000, O/N at 4°C. Membrane was then washed four times in PBS Tween. Anti-mouse-HRP diluted 1:8000 was added to reveal mouse IgGs. After washing, membranes were revealed with ECL.

ELISA for recognition of "coated" or "captured" Fc-EDA1

In two 96 wells ELISA plate, six lines were coated with 100 $\mu$l per wells of goat-anti-human (JIR 109-005-098) at 5 $\mu$g/ml in PBS, five lines were coated with Fc-EDA1 (APO200) at 5 $\mu$g/ml in PBS and five lines were coated with Fc-APRIL-2826 at 5 $\mu$g/ml in PBS. Plates were incubated O/N at 4°C, then blocked for 1 h at 37°C with blocking buffer.

100 $\mu$l/well of Fc-EDA or Fc-APRIL at 2 $\mu$g/ml in incubation buffer were added in lines coated with goat-anti-human. Plates were incubated for 1 h at 37°C and washed three times. In separate tubes, 2-fold dilutions of Renzo2, EctoD1, EctoD2, EctoD3 or Aprily2 starting at 1 $\mu$g/ml (or 8 $\mu$g/ml for EctoD1), were performed.

In the ELISA plate, 100 $\mu$l per well of the different mAbs were added and incubated for 1 h at 37°C. Plates were revealed by 100 $\mu$l per well of HRP-coupled anti-mouse antibody diluted 1:8000 in incubation buffer for 30 min at 37°C. The plates were revealed as needed with 100 $\mu$l per well of OPD solution and reactions were stopped with 50 $\mu$l per well of 2N HCl. The plates were finally read at 492 nm.

Competition ELISA (anti-EDA antibodies block Flag-EDA1 from binding to EDAR-Fc)

A 96 wells ELISA plate was coated O/N at room temperature with 100 $\mu$l per well of EDAR-Fc at 1 $\mu$g/ml in PBS. The plate was then blocked for 1 h at 37°C with blocking buffer.

In separate pre-incubation plates, 2-fold serial dilutions of Flag-EDA1 were performed in incubation buffer, then fixed amounts of antibodies Renzo2, EctoD1, EctoD2, EctoD3, Aprily2 were added so that the first final concentration of Flag-EDA1 was 500 ng/ml, and the final concentrations of antibodies were either 125 ng/ml or 10 $\mu$g/ml. Plates were incubated for 1 h at room temperature.

Of the pre-incubation plate content, 100 $\mu$l were transferred to the ELISA plate. Binding of Flag-EDA1 to EDAR-Fc was revealed with 100 $\mu$l per well of biotinylated anti-Flag M2 mAb, diluted 1:5000 in incubation buffer for 30 min at 37°C, followed by 100 $\mu$l per well of HRP-coupled streptavidin diluted 1:5000 in incubation buffer for 30 min at 37°C. The plates were revealed with 100 $\mu$l per well of OPD solution and reaction was stopped with 50 $\mu$l per well of 2N HCl. The plates were finally read at 492 nm.

Titrations of different Flag-EDA and different Fc-EDA

**Titration:** Two-fold dilutions of Flag-EDA1, Flag-EDA2, Fc-EDA1 and Fc-EDA2 were performed in a pre-incubation plate, so that the first final concentration is 400 ng/ml (or 1:50 for supernatants of unknown concentration).
**ELISA:** One ELISA plate is coated O/N at 4°C with 100 $\mu$l per well of EctoD2 at 1 $\mu$g/ml in PBS. The plate is blocked for 1 h at 37°C with blocking buffer. The content of the pre-incubation plate is transferred in the ELISA plate and incubated for 1 h at 37°C. The binding of EDA to EctoD2 is revealed with 100 $\mu$l per well of biotinylated EctoD3 at 1 $\mu$g/ml for 1 h at 37°C, followed by HRP-coupled streptavidin and OPD.

EctoD2-EctoD3 and Fc sandwich ELISA

1. An ELISA plate was coated with 100 $\mu$l per wells of EctoD2 at 5 $\mu$g/ml in PBS O/N at 4°C. The plate was then blocked for 1 h at 37°C with different block buffers, all in PBS: a) 4% milk, 0.5% Tween-20 b) 4% milk, no Tween, c) 0.5% Tween 20, no milk, d) 2% BSA, 0.5% Tween-20, e) 5% FCS, 0.5% Tween.

   Two-fold dilutions of Fc-EDA1 EDI200, Fc-EDA2 or Fc-FasL were performed in the respective incubation buffer made by diluting blocking buffers 1:10 in PBS, with first final concentrations of 50 ng/ml.

   Fc-EDA1 EDI200 was also titrated in 20% human serum or 5% mouse serum WT or in the presence of 1 $\mu$g/ml fixed concentration of EDAR-Fc or BCMA-Fc.

   In addition, human serum and human serum depleted on EctoD2 at 50% in incubation buffer, 50% FCS and 50% FCS depleted on EctoD2 in incubation buffer, 25% mouse serum in incubation buffer (WT, Tabby, Ove1B), pure DMEM/Nut mix medium 2% FCS, pure 293 cells supernatant, pure 293 cells S/N depleted from EDA (cycled on EctoD2-affinity column), fractions 7-12 of an empty elution of the affinity column, and fractions 7-12 of an elution of the affinity column cycled with 3 L 293 cell supernatant (50 $\mu$l fraction + 50 $\mu$l in buffer, or 10 $\mu$l fraction + 90 $\mu$l incubation buffer) were tested . The plate was incubated for 2 h at 37°C.

   The reaction was revealed with biotinylated-EctoD3, followed by HRP-coupled streptavidin and OPD or TMB solutions. Reactions were stopped with HCl and read at 492 nm for OPD and 450 nm for TMB.
2. An ELISA plate is coated with 100 $\mu$l per well of goat anti-human (JIR 109-005-098) at 5 $\mu$g/ml in PBS O/N at 4°C. The plate was blocked 1 h at 37°C with blocking buffers. Three-fold dilutions of EDI200, Fc-EDA2 Fc-FasL, EDAR-Fc and BCMA-Fc at first final concentrations of 200 ng/ml were performed. Plate was revealed with 100 $\mu$l of goat-anti-human-HRP (JIR 109-035-003) and revealed with 100 $\mu$l per well of OPD solution. Plate was the read at 492 nm.

ELISA for endogenous EDA

To detect endogenous EDA in serum, a sandwich ELISA is performed as follows:

a) Coat 100 $\mu$l/well of EctoD2 at 1 $\mu$g/ml in PBS for 2 h at 37°Cor overnight at room temperature.

b) Block for $\geq$ 1 h in block buffer.
c) Add 100 $\mu$l of pre-depleted human serum (Pascal's) or FCS.
d) Reveal for 1 h at 37°C with 100 $\mu$l biotinylated EctoD3 at 1 $\mu$g/ml in incubation buffer.
e) Add 100 $\mu$l of HRP-coupled streptavidin diluted 1:5000 in incubation buffer for 30 min at 37°C.
f) Add 100 $\mu$l of OPD solution, and wait as required.
g) Stop reaction with 50 $\mu$l of 2 N HCl.
h) Read absorbance at 492 nm.

The pre-depletion of sera (used in point c) is performed in a separate ELISA plate as follows:

i) Coat ELISA plate with 100 $\mu$l/well of depleting or control reagent (EctoD2, Aprily2, EDAR-Fc, XEDAR-Fc, EDAR-Fc+XEDAR-Fc, BCMA-Fc) at 1 $\mu$g/ml in PBS for 2 h at 37°C.
ii) Block for $\geq$ 1 h in block buffer. Add 100 $\mu$l serum and incubate for the indicated time at the indicated temperature.
iii) Transfer serum in the next well, and incubate as indicated. Repeat again if required.
iv) Transfer pre-depleted sera to the ELISA plate coated with EctoD2.
v) The standard curve (APO200) is prepared in saturated wells or the pre-depletion plate as indicated, then transferred in the ELISA plate.

ELISA for endogenous EDA (I)

**Serum depletion:** i) EctoD2 and EDAR-Fc. iii) human serum O/N at 4°C, then 30 min at room temperature, then 30 min at room temperature. vi) Std curve starting at 50 ng/ml and 2-fold dilutions.
**ELISA:** As described in the general protocol.

ELISA for endogenous EDA (II)

**Serum depletion:** i) EctoD2, EDAR-Fc, XEDAR-Fc (Alexis), EDAR-Fc and XEDAR-Fc, BCMA-Fc, Aprily2, PBS. iii) human serum or FCS, in hexaplicates O/N at 4°C, 30 min at room temperature, then 30 min at 37°C. Alternatively, human serum was depleted in duplicate with 3 incubations of 30 min at room temperature. vi) Std curve starting at 2 ng/ml and 2-fold dilutions.
**ELISA:** As described in the general protocol.(with 2-fold dilutions of sera). Inter-plate data were normalized to standard curves.

ELISA for endogenous EDA (III)

**Serum depletion:** i) EctoD2, EDAR-Fc, XEDAR-Fc (Alexis), EDAR-Fc and XEDAR-Fc, BCMA-Fc , Aprily2, PBS. iii) human serum or FCS, in triplicates. Also monoplicates of FCS spiked with 5 ng/ml of Fc-EDA1 or Fc-EDA2. O/N at 4°C, 30 min at room temperature, then 30 min at 37°C. Alternatively, human serum was depleted in duplicate with 3 incubations of 30 min at room temperature. vi) Std curve starting at 2 ng/ml and 2-fold dilutions.
**ELISA:** As described in the general protocol.(with 2-fold dilutions of sera). Include conditions with 100 $\mu$l of WT mouse serum or 100 $\mu$l of Tabby serum.

ELISA for endogenous EDA2

**Serum depletion:** i) EctoD2, XEDAR-Fc, BCMA-Fc-739, PBS. iii) FCS spiked with 15 ng/ml Flag-EDA2 or 15 ng/mml of Flag-EDA2 alone O/N at 4°C, then for 30 min at room temperature, then for 30 min at 37°C.
**ELISA:** As described in the general protocol.

Test of different depletion durations

**Serum depletion:** i) EctoD2, EDAR-Fc and PBS. iii) FCS alone or spiked with 5 ng/ml APO200 for:

1. 30 min at RT
2. O/N at 4°C
3. O/N at 4°C, 30 min at RT
4. O/N at 4°C, 30 min at RT, 30 min at RT
5. O/N at 4°C, O/N at 4°C
6. O/N at 4°C, O/N at 4°C, 30 min at RT, 30 min at RT

**ELISA:** As described in the general protocol.

Validation of XEDAR-Fc batches by ELISA

An ELISA plate was coated O/N at room temperature with 100 $\mu$l per well of XEDAR-Fc Alexis, XEDAR-Fc 1060 (#1011-11), XEDAR-Fc 1060 (#1101-05) or EDAR-Fc at 1$\mu$g/ml in PBS. Plate was blocked with blocking buffer for 1 h at 37°C. Two fold dilutions of Flag-EDA1 (first final concentration 400 ng/ml) or Flag-EDA2 (first final conc 50-fold diluted 20x Opti, #811-06) were added for 1 h at 37°C. Flag-ligands were revealed with biotinylated M2 (100 $\mu$l, 1:5000, 30 min, 37°C) followed by HRP-coupled streptavidin (100 $\mu$l, 1:5000, 30 min, 37°C) and OPD.

## 4.2 Histology

Animals and antibody administration

Wild-type and *EDA*-deficient Tabby mice were treated at weaning (between day 21 and 26) with or without an agonist anti-EDAR monoclonal mouse IgG1 antibody (mAbEDAR3), administered intraperitoneal at 2 mg/kg. Treatment was then repeated every two weeks. Mice were sacrificed after 12 weeks of treatment (36). These mice were used for an experiment unrelated to the subject of this master thesis (37), for which skin, eyelids and salivary glands were used. In this study, these mice were used to study the remaining glands of the head.

Histology sections

Four mice (wild type ± mAbEDAR3, Tabby ± mAbEDAR3) were fixed in formalin, with their abdomen opened and intestine put outside to improve fixation. Heads were decalcified for three hours in a decalcifying solution (decalcifier II, Surgipath). Heads were then dehydrated, processed and embedded in paraffin. After 10 minutes decalcification, 3 $\mu$m thickness slides

were sectioned. Coronal sections were made through heads of the sixteen weeks-old mice. After drying, slides were stained with haematoxylin and eosin and cover-slipped.

Pictures of slides were taken using a light microscope (Zeiss-Axioplan) equipped with a ProgRes C5 digital camera. Low magnification pictures were taken with the macro mode of a digital camera.

# 5 Results

## 5.1 ELISA

### 5.1.1 Characterization of anti-EDA antibodies

*EDA*-deficient Tabby mice were immunized with an active recombinant form of EDA1, Fc-EDA1, to generate blocking anti-EDA1 antibodies. Three EDA-specific hybridomas were obtained. Antibodies produced by these hybridomas, named EctoD1, EctoD2, and EctoD3, were all of mouse IgG1 isotype. Purified antibodies (Fig. 3A) were tested for their ability to recognize denatured and native EDA1. EctoD1 and EctoD2 weakly recognized reduced Fc-EDA, but also slightly cross-reacted with Fc-APRIL by Western blot (Fig. 3B). EctoD3 produced a stronger and specific signal, but that remained weaker than that obtained with Renzo2, the commercial anti-EDA antibody (Fig. 3B). An ELISA assay was performed in which the Fc-EDA1 was either coated directly on the plate, a procedure that partially denatures proteins, or captured via its Fc portion to preserve its native conformation. Renzo2 recognized coated Fc-EDA1 better than captured Fc-EDA1, suggesting that it preferentially recognizes denatured EDA1. In contrast, EctoD1, EctoD2, and EctoD3 all recognize coated and captured Fc-EDA1 with similar signal efficiency, suggesting that they recognise surface-exposed epitopes in EDA1 (Fig. 3C).

### 5.1.2 EctoD2 and EctoD3 prevent the interaction of EDA1 with EDAR

As anti-EDA antibodies appeared to recognize surface-exposed epitopes, we tested whether they would interfere with the binding of EDA1 to EDAR. For this purpose, the binding of titrated amounts of Flag-EDA1 to coated EDAR-Fc was tested in an ELISA assay, in the presence or absence of a fixed amount of anti-EDA antibodies. Although EctoD1 and Renzo2 did not interfere with the EDA1-EDAR interaction, an excess of EctoD2 and EctoD3 inhibited the interaction (Fig. 4). This suggests that EctoD2 and EctoD3 might be function-blocking antibodies.

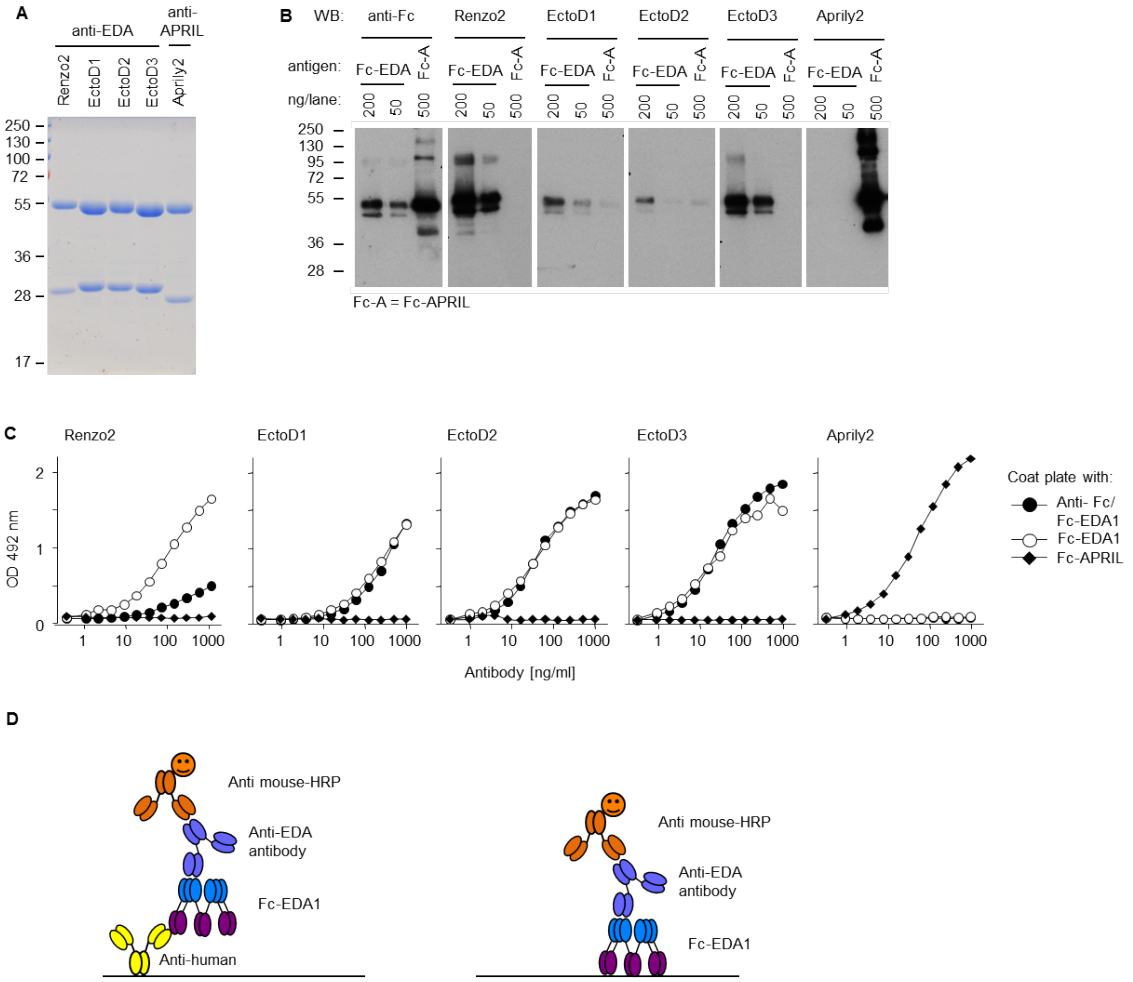


Figure 3: **Anti-EDA antibodies recognize epitopes on native EDA1.** A, SDS-PAGE analysis and Coomassie Blue staining of 10 $\mu$g/lane of the indicated purified mouse IgG1 monoclonal antibodies under reducing conditions. Migration positions of molecular mass standards (in kDa) are shown. B, Fc-EDA1 (200 or 50 ng) and Fc-APRIL (Fc-A, 500 ng) were resolved by Western Blotting (WB) under reducing conditions and revealed with anti-human immunoglobulin (anti-Fc), anti-EDA (Renzo2, EctoD1, EctoD2, EctoD3), or anti-APRIL (Aprily2) antibodies. C, Purified Fc-EDA1 and Fc-APRIL proteins were coated directly in an ELISA plate. Fc-EDA1 was also captured via the Fc portion using an anti-human antibody. Coated proteins were revealed with the indicated antibodies at the indicated concentrations. D, Experimental design of the ELISA shown in panel C.

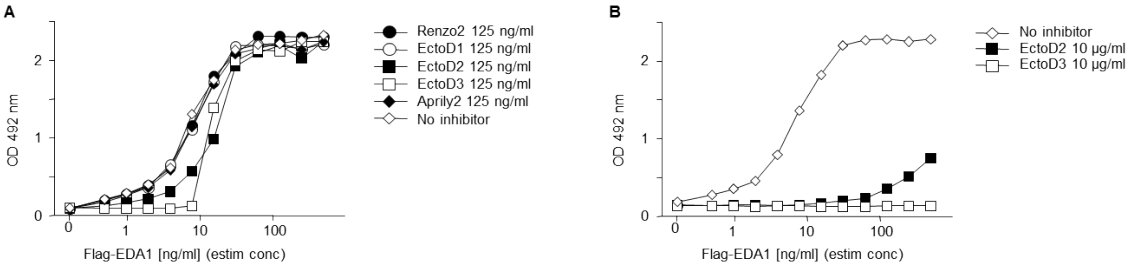


Figure 4: **Anti-EDA antibodies EctoD2 and EctoD3 inhibit EDA1.** A, Flag-EDA1 was diluted at the indicated concentrations and preincubated with or without anti-EDA (Renzo2, EctoD1, EctoD2, or EctoD3) or anti-APRIL (Aprily2) monoclonal antibodies at a fixed concentration of 125 ng/ml. The binding of Flag-EDA1 to coated EDAR-Fc protein was then probed by an ELISA essay. B, The same ELISA essay is performed with or without 10 $\mu$g/ml of anti-EDA (EctoD2, or EctoD3) monoclonal antibodies competitor.

### 5.1.3 Sensitive detection of Fc-EDA by sandwich ELISA

In different animal models of HED, pre- and post-natal treatments with Fc-EDA1 could reverse several aspect of the disease. Because recombinant Fc-EDA1 is currently tested in clinical trials, it is important to be able to detect its presence in serum for the monitoring of its pharmacologic parameters. Thus, anti-EDA antibodies Renzo2, EctoD1, EctoD2 and EctoD3 were tested in different conditions to evaluate their ability to recognize Fc-EDA1 in a sandwich ELISA. The most sensitive combination was found to be EctoD2 at capture, and biotinylated EctoD3 for revelation (data not shown) (35).

The pair of antibodies EctoD2 and EctoD3 could detect Fc-EDA1 and Fc-EDA2 at less than 1 ng/ml (Fig. 5A), yet did not recognize the negative control Fc-FasL (Fig. 5B). We therefore further characterized this pair of antibodies.

The recognition of Fc-EDA1 using the EctoD2/EctoD3 sandwich ELISA was not decreased when Fc-EDA1 was pre-incubated with a vast excess of the recombinant receptor EDAR-Fc, indicating that the sandwich ELISA recognizes both free and receptor-bound EDA1 (Fig. 5C). In fact, the presence of EDAR-Fc slightly increased the signal, even when EDAR-Fc was added alone in the ELISA, in the absence of Fc-EDA1 (Fig. 5C). This could be explained if recombinant EDAR-Fc is already partially loaded with EDA. Because EDAR-Fc was produced in mammalian cells, in the presence of FCS, the background might be caused by the presence of endogenous bovine EDA in foetal calf serum.

To improve the sensitivity of the EctoD2/EctoD3 sandwich ELISA, we measured detection of Fc-EDA1 in the presence of various block and incubation buffers, and also tested two different peroxydase substrates (OPD and TMB). TMB gave a stronger revelation signal, but OPD gave less background (Fig. 5D). The different blocking solutions were all relatively equivalent, with the exception of the FCS-based blocking solution that gave a significant signal, even in the absence of any Fc-EDA1 (Fig. 5E). The signal obtained in the presence of FCS could be explained by the presence of endogenous EDA in FCS. In conclusion, we used chose to work with OPD as revelation substrate and with our regular milk- and Tween-20-containing buffer for subsequent experiments.

As one aim of the EDA ELISA is to monitor Fc-EDA1 in mouse or human serum, and as it is known that serum can interfere with many ELISA tests, we tested the effect of human and mouse serum on the detection of Fc-EDA1 in the sandwich ELISA. 5% of mouse serum or 20% of human serum did not interfere with the detection of Fc-EDA1 in the sandwich ELISA, except that human serum generated a signal on its own (Fig. 5F). This indicates first that the presence of 5 or 20% serum does not quench the signal, and second that human serum might contain endogenous levels of EDA that is detected by the EctoD2/EctoD3 sandwich ELISA.

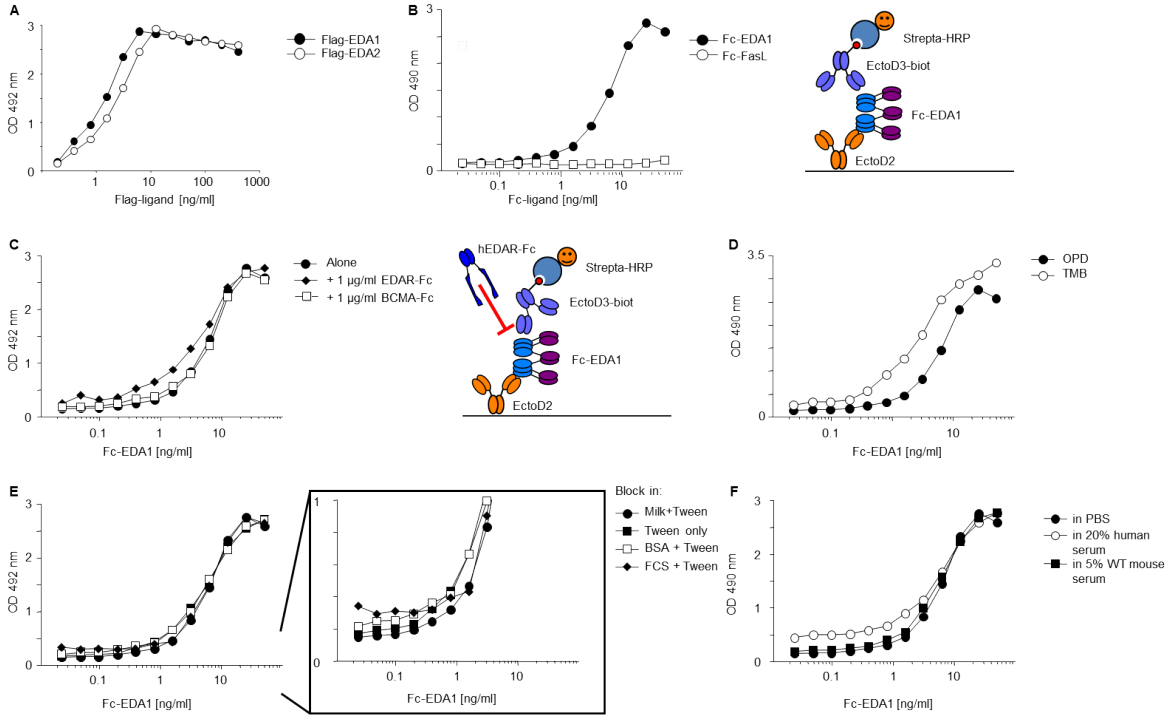


Figure 5: **Sensitive detection of EDA by sandwich ELISA.** A and B, Sandwich ELISA for EDA1 and EDA2 (Flag-EDA1, Flag-EDA2, Fc-EDA1, and Fc-EDA2) is performed using anti-EDA EctoD2 at capture and biotinylated anti-EDA EctoD3 for detection. Biotinylated antibodies were revealed with HRP-coupled streptavidin. C, EctoD2/EctoD3-biot sandwich ELISA performed as in panel A , but in the presence of a fixed concentration (1 $\mu$g/ml) of EDAR-Fc or BCMA-Fc. D, Comparison of different revelation solutions (OPD and TMB) for the EctoD2/EctoD3-biot sandwich ELISA. E, Comparison of different blocking solution with indicated composition for the EctoD2/EctoD3-biot sandwich ELISA. F, Recognition of Fc-EDA1 in the EctoD2/EctoD3-biot sandwich ELISA performed in 20% human serum or in 5% mouse serum.

### 5.1.4 Detection of endogenous EDA

Because of the "background" observed in the ELISA performed in the presence of FCS or human serum, we explored the possibility that endogenous EDA might be present in serum and might be detected with the EctoD2/EctoD3 sandwich ELISA. For this purpose, we thought to pre-deplete sera from endogenous EDA, and then perform the sandwich ELISA. A pre-depletion with EctoD2 should abolish the signal, unless the observed signal is a background unrelated to the presence of EctoD2 in the ELISA plate. A pre-depletion with EDAR-Fc or XEDAR-Fc should deplete EDA1, respectively EDA2 in the serum by mechanisms distinct from the specificity of EctoD2, and therefore provide convincing hints about the true nature of the signal.

We first tested that EDAR-Fc and XEDAR-Fc could respectively bind EDA1 and EDA2 in an ELISA assay (Fig. 6), and were therefore suitable for pre-depletion of serum. EDA was detected in foetal calf serum and human serum, but not in mouse serum (WT or Eda-deficient), for reasons that are unclear (Fig. 7A). Pre-depletion of human serum or FCS on irrelevant control proteins (BCMA-Fc, Aprily2) did not abolish the signal in the ELISA; but pre-depletion on EctoD2 fully and reproducibly removed all signal (Fig. 7B,C). This indicates that signal (whether specific or not) is indeed mediated by something captured

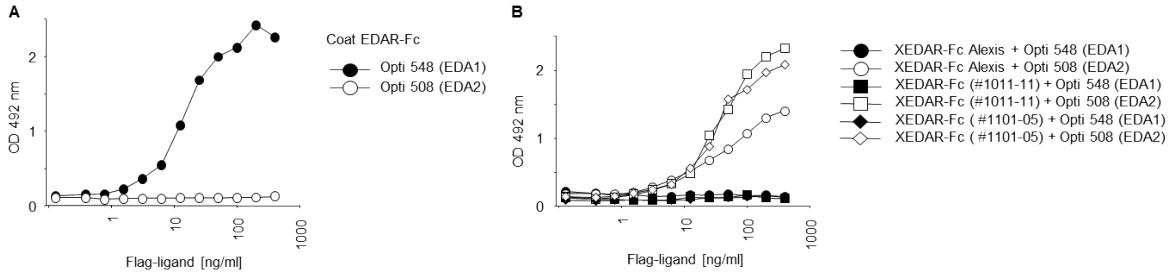


Figure 6: **Specific binding of EDA1 to EDAR and EDA2 to XEDAR.** The indicated receptors-Fc were coated in an ELISA plate, and revealed with titrated amounts of Flag-EDA1 or Flag-EDA2, followed by anti-Flag M2-biot and HRP-coupled streptavidin. A, EDAR-Fc specifically binds to Flag-EDA1. B, Different preparations of XEDAR-Fc proteins specifically recognize Flag-EDA2.

by EctoD2. Interestingly, about half of the signal was also depleted by pre-incubation on immobilized EDAR-Fc (Fig. 7C,D), indicating that at least some of the signal detected in the EctoD2/EctoD3 sandwich ELISA is due to a form of EDA1 able to bind to EDAR. The remaining of the signal was apparently not due to EDA2, as pre-depletion on XEDAR-Fc did not affect the signal. We confirmed the efficiency of the pre-depletion procedure with EDAR-Fc or XEDAR-Fc in the presence of serum using serum spiked with recombinant EDA1 or EDA2, and found that pre-depletion of spiked EDA1 with EDAR-Fc and of EDA2 with XEDAR-Fc was efficient (Fig. 7D,E). In all of these pre-depletion experiments, sera were depleted overnight, followed by two further depletions of 30 min each. We found that a single depletion of 30 min was insufficient for efficient depletion of endogenous EDA in FCS, but that a single overnight incubation was already sufficient for depletion (Fig. 8).

Taken together these experiments indicate that i) the EctoD2/EctoD3 sandwich ELISA specifically recognizes endogenous EDA in human and foetal calf sera, ii) that part of this EDA is competent to bind to EDAR, iii) that even in conditions allowing depletion, a fraction of the signal does not bind EDAR-Fc or XEDAR-Fc. This may be denatured EDA, receptor-bound EDA, or a non-specific signal.

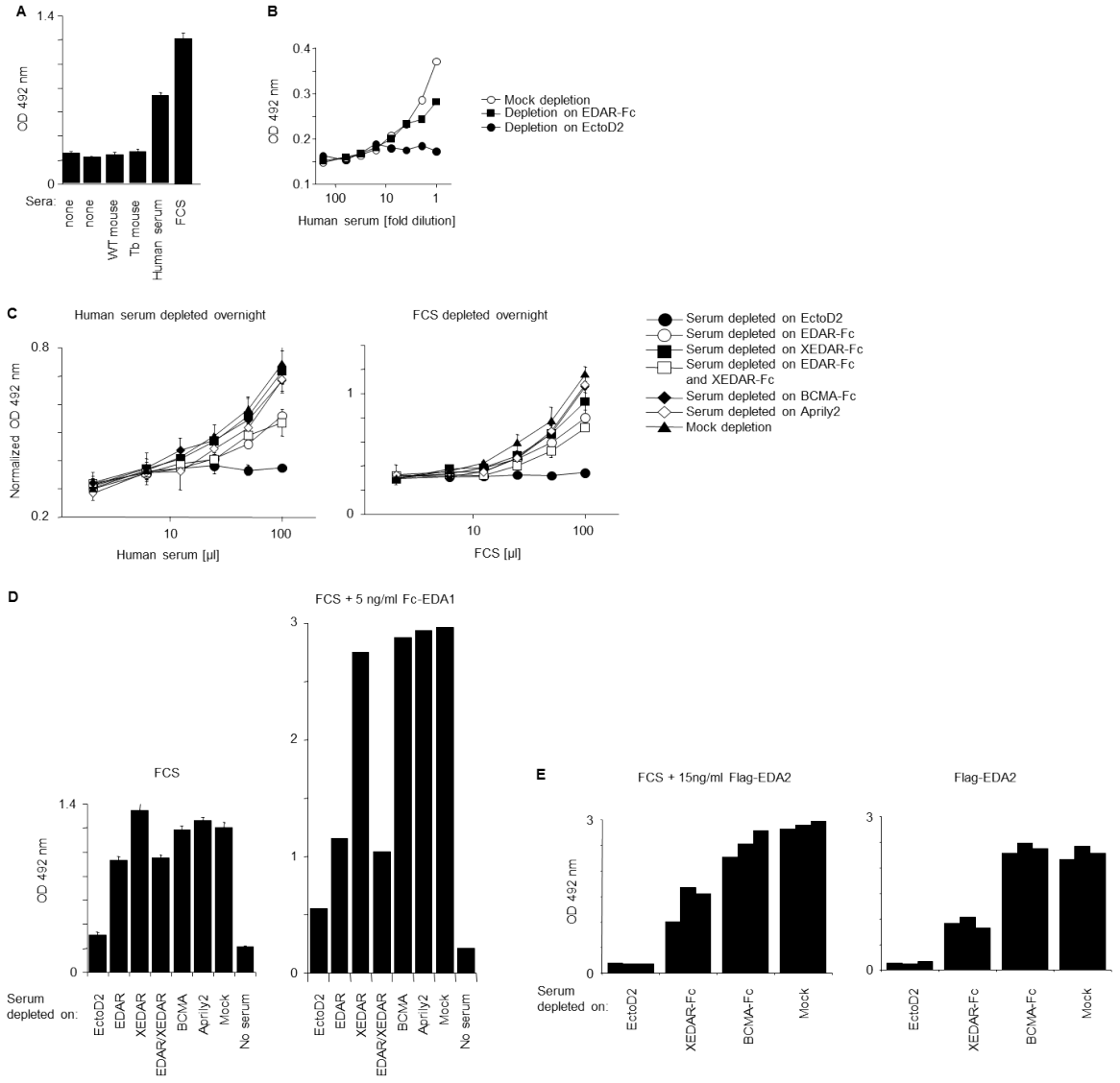


Figure 7: **ELISA for the detection of endogenous EDA.** A, Detection of EDA by sandwich ELISA (EctoD2 and biotinylated EctoD3) in fetal calf serum (FCS), human serum, and Tabby and wild type mouse sera. B, Human serum was depleted on either anti-EDA EctoD2 mAb or EDAR-Fc coated ELISA plates. Serial dilutions of depleted sera were then analysed by EctoD2/EctoD3-biot sandwich ELISA. C, Human serum and fetal calf serum (FCS) were pre-depleted in 6-plicates as indicated, then serial dilutions of depleted sera were analysed by EctoD2/EctoD3-biot sandwich ELISA. D, Fetal calf serum (FCS) and FCS spiked with 5 ng/ml of Fc-EDA were depleted according to the indicated conditions, then analysed by EctoD2/EctoD3-biot sandwich ELISA. E, Flag-EDA2 at 15 ng/ml in incubation buffer or in FCS was depleted in triplicate on indicated proteins, then analyzed by sandwich ELISA.

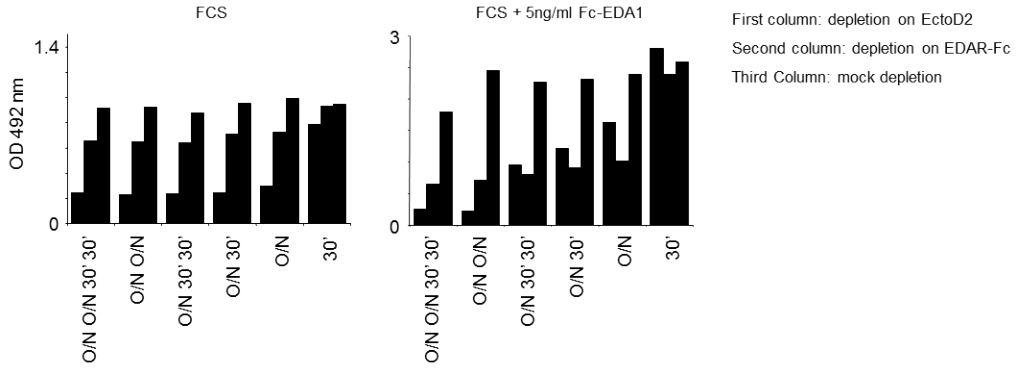


Figure 8: **Time required for efficient pre-depletion of endogenous EDA.** Fetal calf serum (FCS) alone or spiked with 5 ng/ml of Fc-EDA1 was depleted for the indicated depletion periods. For each of the conditions, 3 bars are shown. The first one represents depletion on the anti-EDA antibody EctoD2, the second column represents depletion on EDAR-Fc, and third column represents undepleted mock-depleted serum. Depleted sera were subsequently analyzed by EctoD2/EctoD3-biot sandwich ELISA.

## 5.2 Histology

### 5.2.1 Localisation of the nasal, lacrimal, and ceruminous glands

The mouse nasal cavity contains numerous constant, symmetrical glands that can be divided in three important groups: lateral, medial and infraseptal. The following paragraphs describe the localisation of these different glands in a wild-type mouse.

The **glandulae nasales laterales** are a large group of glands situated in the lateral wall of the nose on the inferior and superior maxillary turbinelle and the nasal duct. They also occupy the anterior and inferior part of the maxillary sinus mucosa. During embryonic development, lateral glands form one after the other and have been numbered from I to VIII in the order in which they arise. Finally all glands form a common glandular mass. The main gland of this group is Steno's gland, number I, that appears at E14. The **glandulae nasales mediales** are located in the inferior part of the nasal septum in the respiratory mucosa. Glands I-III constitute a common glandular mass on the nasal septum mucosa between the vomeronasal (Jacobson's) organ and the olfactory region. Gland IV has an isolated location in the inferior part of the nasal septum and frontwards of the vomeronasal organ. They appear at E14-15. The **glandulae nasales infraseptales** are situated beneath the anterior part of the nasal septum in a space between both maxillas. Four glands, developing at E14-15, form a common gland. The glandulae anterior organi jacobsoni is located on the anterior upper edge of the vomeronasal organ and forms at E15. This gland is fused to the medial glands. The **glandulae propria sinus maxillaris** resides in the maxillary sinus and arises at E14. Lateral and maxillary glands have no defined limits. **Bowman's glands**, typical of the olfactory region, are located between the olfactory nerves and develop at E17. The **glandulae nasopharyngeae** are located in muscles on the posterior part of the nasopharynx and develop at E17 (38,39).

Coronal head sections were made at different depths, as indicated (Fig. 9). The glandulae nasales laterales and medialis (Fig. 10) were quite easy to find in the lateral and medial walls of the nasal cavity, respectively, just beneath the mucosa. Some glandular ducts were also

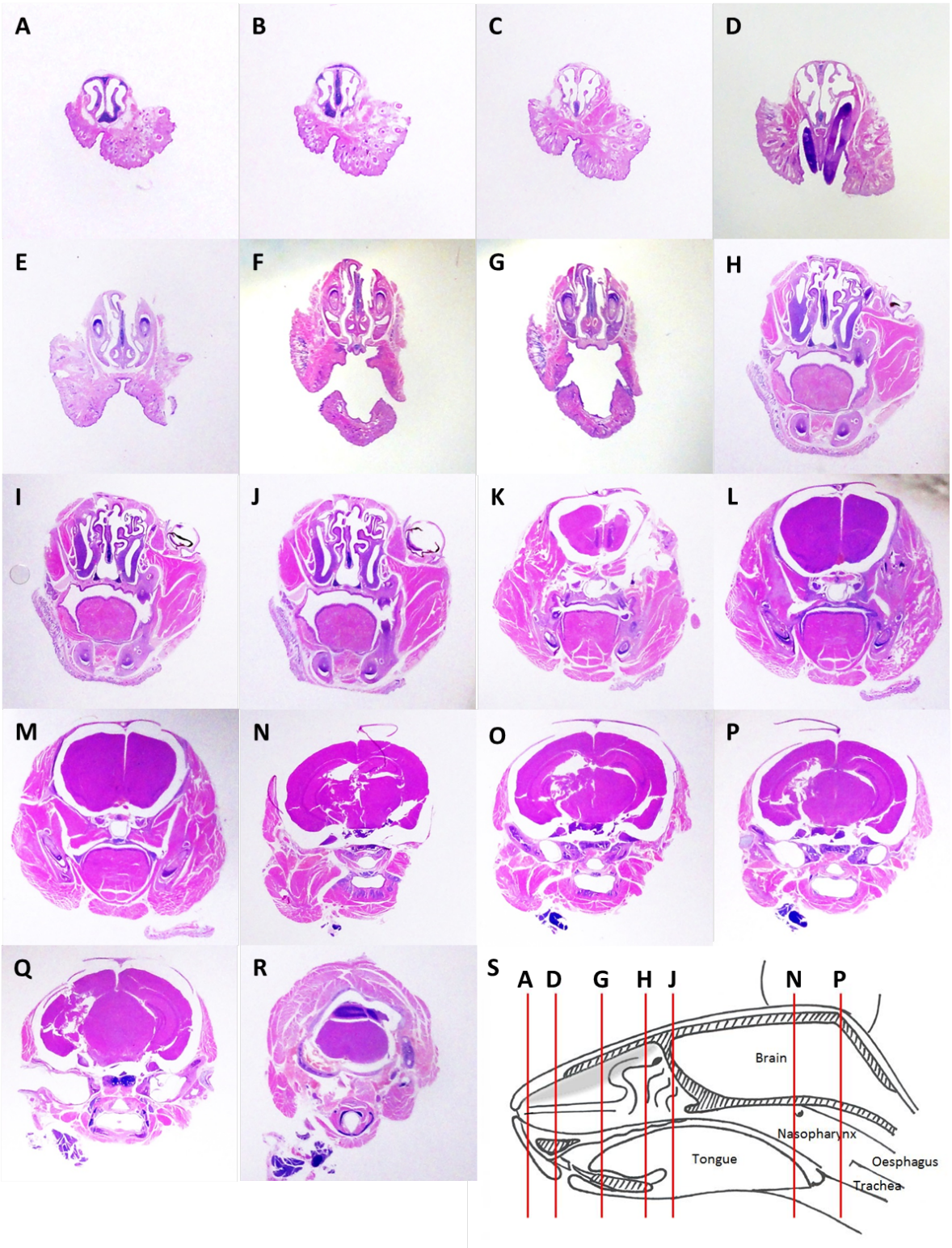


Figure 9: **Coronal sections of the head of a wild-type mouse.** A - R, H&E stained coronal sections of the head cut at different levels. S, Scheme of a mouse head showing the positions of sections shown in panels A, D, G, H, J, N and P.

visible in these sections. In contrast, the different glands, numbered from I to VIII for the lateral glands and from I to IV for the medial glands, were impossible to distinguish. In the same way, glandulae anterior organi jacobsoni could not be differentiated from the medial group. In their works, Broman (1921) and Grüneberg (1971) followed the glandular development though different embryonic ages and were thereby able to distinguish and number the different glands at their respective locations. The gland occupying the sinus maxillaris (Fig. 10) was also easy to find in the sinus just beneath the mucosa, but its boundary with the lateral group was not clear. The infraseptal gland (Fig. 10) could be found in the area described above, but there was no structural evidence that it developed from four different glands. Bowman's glands were small cells bundles located beneath the olfactory epithelium in-between the olfactory nerves. (Data not shown: no good pictures of these glands could be taken because of the small size of the structures.) In the nasopharynx, large heaps of nasopharyngeae glands could be found just below the superior mucosa of the nasopharynx in between muscle fibres. This group of gland was not found in all analysed mice because of technical difficulties.

Concerning the ear, there are three important glandular groups. The **glandulae mucosae tubae auditivae** is situated in the region next to the Eustachian tube and the nasopharynx. The **glandula ceruminosa** is a single large ear-wax gland and its duct opens into the external auditory meatus near the tympanic membrane. This gland first arises at E14.5. The **sebaceous glands** are associated to fine hairs in the external auditory meatus. They appear at day 3 post-birth in mice (38,39).

The Eustachian tube region and its associated gland (Fig. 10) were recognised with no effort, the main difficulty was to get coronal section through this area. Concerning the ceruminosa gland (Fig. 10), it is a large gland located beneath the external auditory meatus and in a lateral position to the head. This gland was found easily. Sebaceous glands in the external auditory meatus were not so easy to find, again because of technical limitations.

Eyeball lacrimal glands are mostly located in the orbit with the exception of the extraorbital lacrimal gland. The **Harderian gland** is located behind the eyeball. It first develops at E14. The **extraorbital lacrimal gland** is located subcutaneously in front of and below the ear. The gland first arises at E14. The **intraorbital lacrimal gland** is located ventral to the eyeball. It develops around the time of birth. The **Meibomian glands**, also named glandulae tarsales, are eyelid glands. These glands start to develop at E17 (38,39).

The harderian gland (Fig. 10) is probably the easiest lacrimal gland to find, just behind the eyeball where it forms a large glandular structure. The extraorbital, intraorbital, and Meibomian glands were not found probably because of their lost in the dissection of the salivary glands. However, fragments of the intraorbital gland could probably be found in the lateral and inferior region to the eyeball.

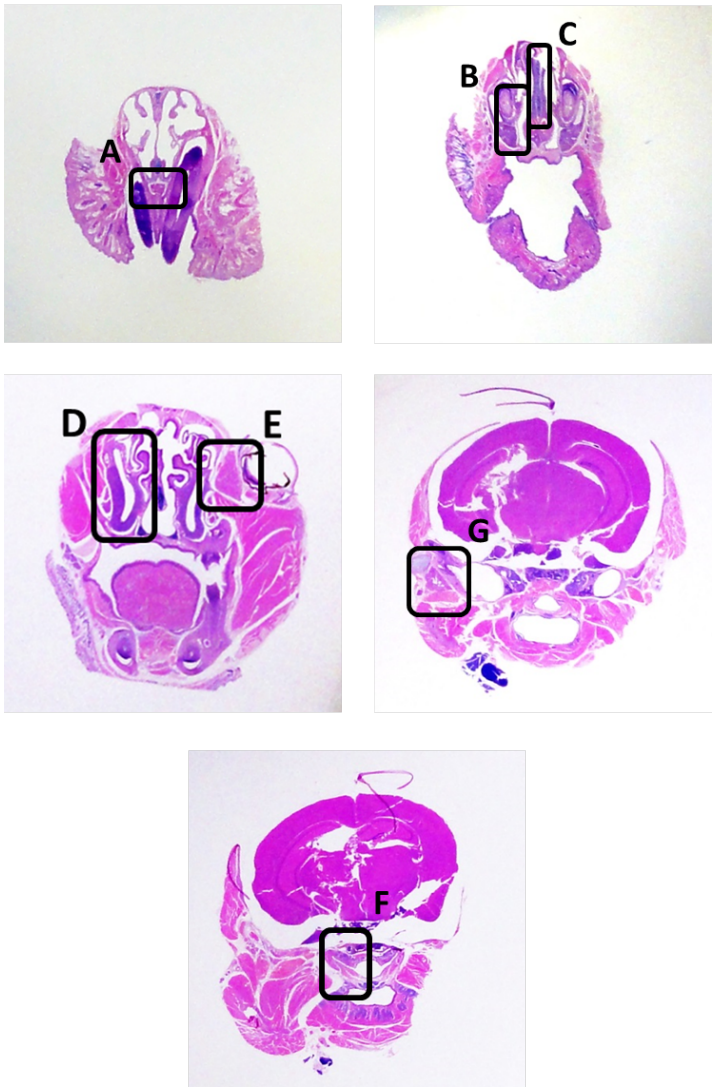


Figure 10: **Location of the main nasal, lacrimal and ceruminous glands.** Important glands are highlighted on five representative sections (see Fig. 9, panels D, G, J, N and P). The glandulae nasales infraseptales (rectangle labelled "A") are located beneath the anterior part of the nasal septum in a space between both maxilla. The glandulae nasales laterales (rectangle "B") are positioned in the lateral wall of the nose on the inferior and superior maxillary turbinelle and the nasal duct. They also occupy the anterior and inferior part of the maxillary sinus mucosa. The glandulae nasales mediales (rectangle "C") are located in the inferior part of the nasal septum in the respiratory mucosa. The glandulae propria sinus maxillaris (rectangle "D") reside in the maxillary sinus. The Harderian gland (rectangle "E") is located behind the eyeball. The glandulae mucosae tubae auditivae (rectangle "F") is situated in the region next to the Eustachian tube and the nasopharynx. The glandula ceruminosa (rectangle "G") is a large gland located beneath the external auditory meatus.

### 5.2.2 Nasal, lacrimal, and ceruminous glands in the *EDA*-deficient Tabby mouse

After finding the glands in wild-type mice, localisation in the EDA-deficient mouse had to be studied. Lateral (Fig. 11), medial (Fig. 12) and sinus maxillaris (Fig. 13) glands could be found in both wild-type and Tabby mice. In his paper of 1970, Grüneberg described the medial glands as missing in Tabby (39). The infraseptal gland (Fig. 14) was missing in the Tabby mouse; in fact the glandular tissue was replaced by loose connective tissue so called "ghost gland" by Grüneberg (1970). The glandula ceruminosa seemed to be composed of less glandular tissue and to have a larger lumen in Tabby. The glandulae mucosae tubae auditivae was not found in any Tabby mice, probably because this structure is absent, as described by Grüneberg (1970). But as the Eustachian tube was not observed on the histology sections of the Tabby mouse, it is not possible to comment about the presence or absence of this gland. Harderian glands (Fig. 15) were observed in Tabby mouse, but their structures, instead of being glandular, were composed of loose connective tissue, as seen for infraseptal glands. Melanocytes that are characteristic the Harderian gland were however present.

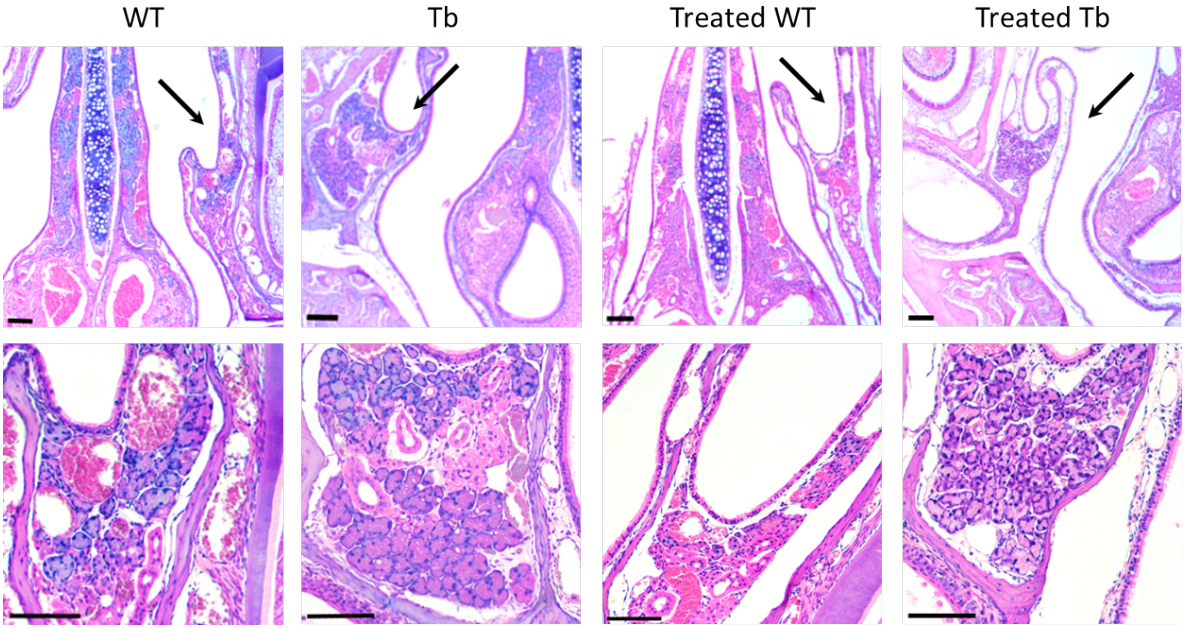


Figure 11: **Glandulae nasalis lateralis in WT and Tabby mice ± mAbEDAR3 treatment.** Top panels : H&E stained sections corresponding to the region shown in rectangle "B" of Fig. 10. Arrows point at the region of interest. Lower panels : enlargement of the region of interest. Scale bar : 100 $\mu$m.

### 5.2.3 5.2.3. Nasal, lacrimal, and ceruminous glands response in mice treated with an EDAR agonist

A potential response of glands in the nasal cavity to an EDAR agonist was analysed. For this purpose, WT and Tabby mice at weaning were treated every two weeks for 12 weeks by intraperitoneal injections of an agonist anti-EDAR antibody. It was clear that nasal, lacrimal, and ceruminous glands that were absent in Tabby mice were still absent in treated adult Tabby mice. We expected to possibly observe an enlargement of the remaining glands in Tabby mice

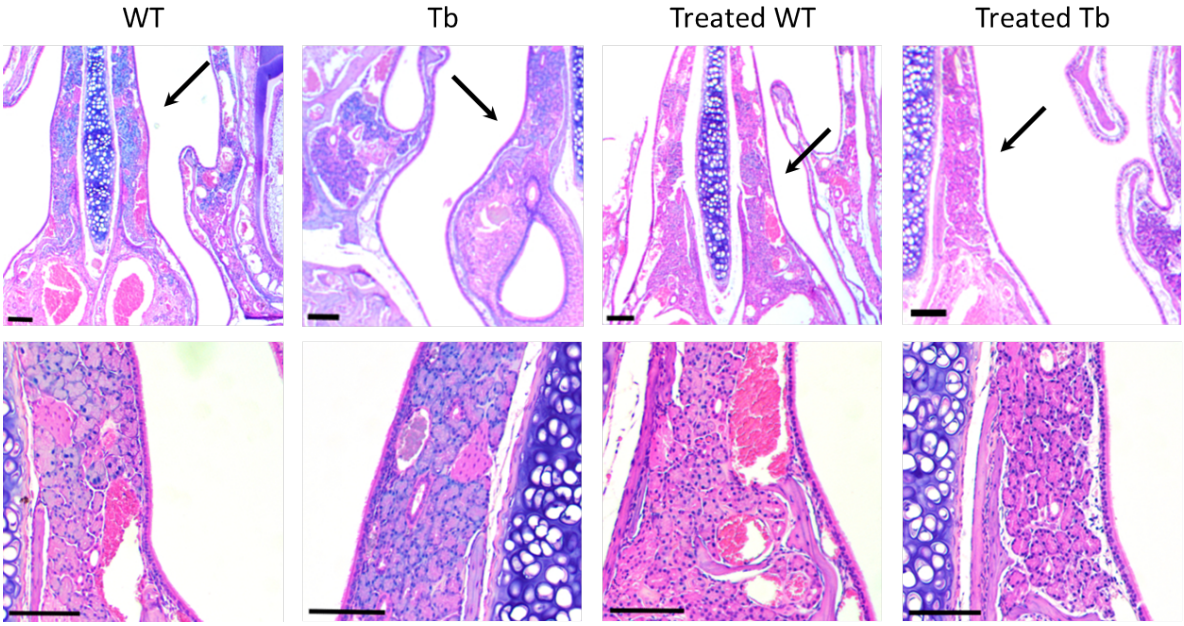


Figure 12: **Glandulae nasalis medialis in WT and Tabby mice ± mAbEDAR3 treatment.** Top panels : H&E stained sections corresponding to the region shown in rectangle "C" of Fig. 10. Arrows point at the region of interest. Lower panels : enlargement of the region of interest. Scale bar : 100 $\mu$m.

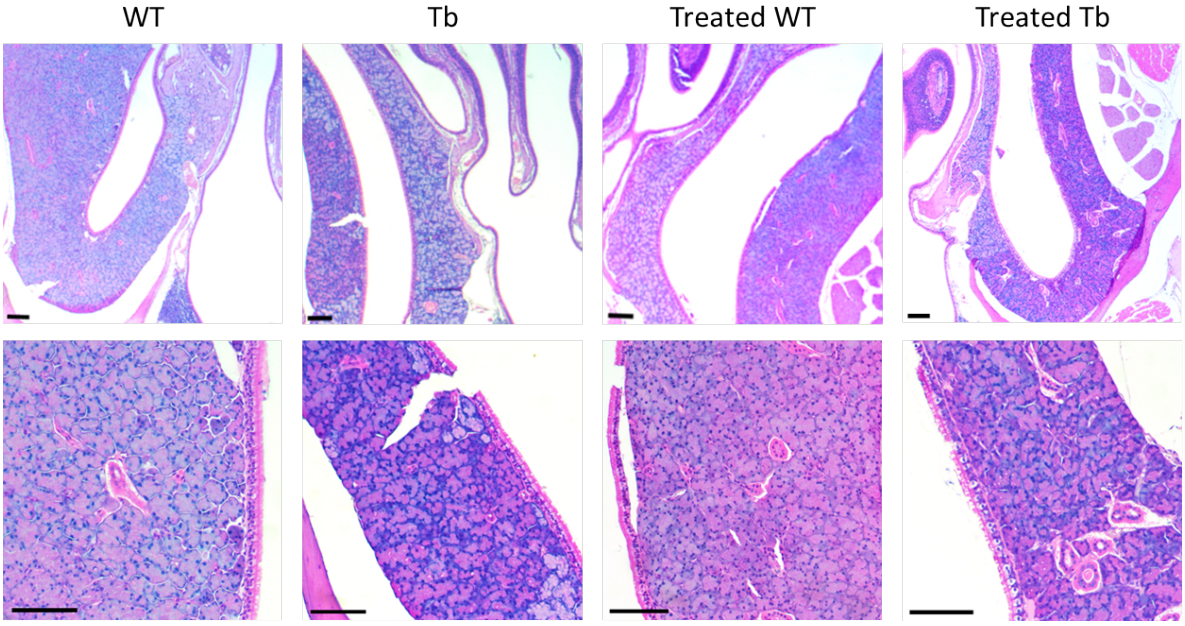


Figure 13: **Glandulae propiae sinus maxillaris in WT and Tabby mice ± mAbEDAR3 treatment.** Top panels : H&E stained sections corresponding to the region shown in rectangle "D" of Fig. 10. Lower panels : enlargement of the region of interest. Scale bar : 100 $\mu$m.

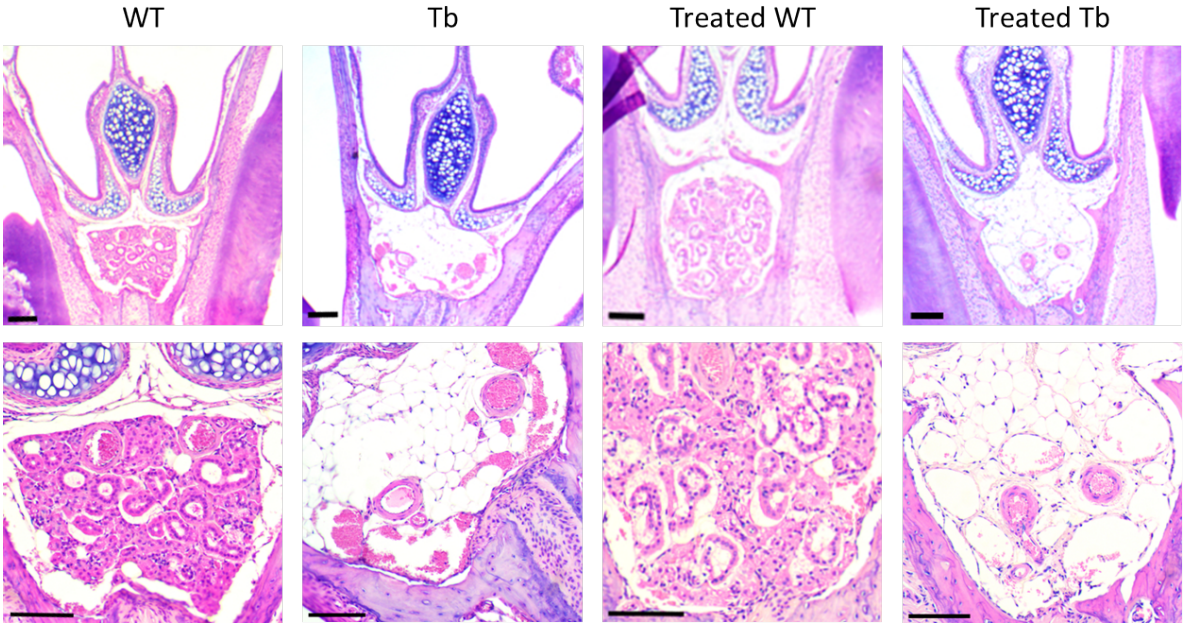


Figure 14: **Glandulae nasalis infraseptalis in WT and Tabby mice ± mAbEDAR3 treatment.** Top panels : H&E stained sections corresponding to the region shown in rectangle "A" of Fig. 10. Lower panels : enlargement of the region of interest. Scale bar : 100 $\mu$m.

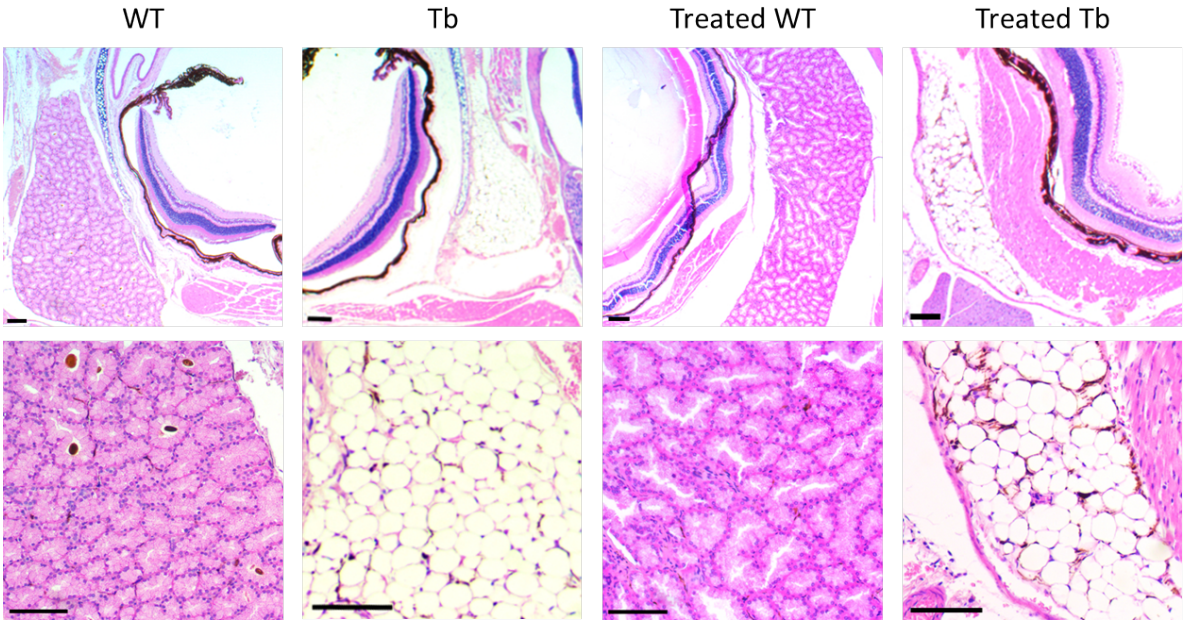


Figure 15: **Harderian gland in WT and Tabby mice ± mAbEDAR3 treatment.** Top panels : H&E stained sections corresponding to the region shown in rectangle "E" of Fig. 10. Lower panels : enlargement of the region of interest. Scale bar : 100 $\mu$m.

upon treatment, as previously observed for sebaceous glands (37). In the treated mice, we didn't notice major phenotypic effects of EDA agonist treatment. However, it is possible that more subtle effects did take place. For example, some glands appeared to have larger number of nuclei in the presence of the agonist, even if this effect remains to be quantified. Further studies using other staining and analysis methods should be performed to see assess in more details whether the treatment in adult mice has a real impact on these glands.

# 6 Discussion

The EDA signalling pathway is essential for proper skin development; indeed, its alteration by mutations leads to loss or altered development of part of ectoderm-derived structures. The implication of EDA in the early development has been intensively studied, but it is known that EDA is also expressed in adults, with potential post-developmental homeostatic roles that need to be specified. Monoclonal antibodies are now available that allow activation or suppression of the EDA pathway at any stage of development (40).

EDAR can be activated in vitro and in vivo either by recombinant EDA1 (Fc-EDA1) or by anti-EDAR agonist antibodies (e.g. anti-EDAR mAb 3) (13,14,36).

Administration of recombinant Fc-EDA1 protein to pregnant Eda-deficient mice permanently rescued the tabby phenotype in the progeny. Treatment given after birth partially reverted the phenotype in both mouse and dog models of XLHED (13,14). In a recent study, Fc-EDA1 was administered to Tabby foetuses by intra-amniotic injections. Reversal of the XLHED phenotype through this route of administration was excellent, with minimal maternal exposure to the drug (41). Recombinant Fc-EDA1 protein replacement therapy of EDA-deficient animal models brings hope for the treatment of HED patients.

Agonists anti-EDAR monoclonal antibodies, when administered in utero to mice or after birth to dogs, also reverted several HED phenotype features (36). Furthermore, adult Eda-mutant mice treated with these antibodies showed normalisation of sebaceous gland size and function. This effect was maintained as long as a chronic treatment was maintained, but reversed after treatment cessation. By acting on sebaceous glands, EDAR agonists could improve skin dryness and eczema frequently observed in HED patients (37,42). In contrast, an inhibition of EDA might be beneficial to different conditions like acne or seborrhea where glandular activity is deregulated.

With regard to the inhibition of the EDA pathway, anti-EDA blocking antibodies, like EctoD2 and EctoD3, are able to supress the action of the recombinant Fc-EDA1 protein. These blocking antibodies, when administered to pregnant wild-type mice, induced HED in their progeny, indicating that they can also inhibit endogenous EDA (35). These blocking antibodies are precious tools to study the developmental and post-developmental roles of the EDA pathway.

As mentioned above, EDAR agonist treatment is effective not only on embryonic tissues but also on adult tissues, at least on sebaceous glands (37). The treatment that was successful to stimulate sebaceous glands in adult mice was performed in this master thesis, but we couldn't demonstrate an effect on the glands studied in this report. There are two possible explanations for this negative result. First, the glands studied do not respond to the treatment in the adult, and second the method used was not efficient enough to produce a detectable effect. Further studies with more elaborated analysis and quantification methods have to be performed. The volume of the gland should also be monitored, for example by serial sections or by extrapolation from a few slides.

An agonist treatment given at the right place and at the correct time of development should induce the formation of structures that are otherwise absent in XLHED. On the contrary, if given after development, no effect should be expected. Sebaceous glands are reduced in tabby mice (39) and respond to the agonist treatment (37,42). As treatment with the agonist had no detectable effect on the "ghost" glands, it is tempting to conclude that there is no residual

glandular tissue in these ghost glands.

The mammary gland is another gland affected in the EDA-deficient Tabby mouse, which produces less amounts of milk (Sonia Schuepbach, personal communication). Unlike other glands, the mammary gland undergoes three different periods of development: the embryonic, puberty and lactation periods. A treatment with EDAR agonists during puberty, pregnancy or lactation has the potential to improve mammary gland function, should EDA be involved at these stages of development.

The development of a potential treatment for HED requires knowing at which point of development a particular structure can respond to a particular dose of treatment. If a structure fully develops in the early developmental stages, treatment has to be started as soon as possible, but on the contrary, if a structure needs a homeostatic stimulation by EDA, treatment could be initiated later. Further studies using antibodies that permit activation and suppression of the EDA pathway at any stage of development will probably answer these questions.

In the sandwich ELISA, two anti-EDA antibodies, EctoD2 and EctoD3 allowed detection of recombinant EDA in buffer and serum. This could be helpful to measure, for example, levels and distribution of recombinant EDA protein in clinical trials. Because we observed that serum alone gave a signal in the ELISA, and that this signal could decreased by pre-depletion on EDAR-Fc, we think that the ELISA can detect endogenous EDA in serum. However, no signal was obtained when mouse serum was assayed. There are several possible explanations for this observation. First, mouse EDA is perhaps not recognized in the ELISA. This seems unlikely since the Eda gene is highly conserved in evolution and furthermore the in vivo blocking assays are working (35). Second, circulating levels of EDA in mice could be lower than in human serum or FCS. For example, most EDA may remain trapped in tissue without access to serum in mice. Finally, mouse serum may contain an inhibitory activity that inhibits the ELISA. There is however currently no evidence for such an inhibitory activity, and Fc-EDA1 was still recognized well in the presence of mouse serum.

The sandwich ELISA could not only be helpful to assess the pharmacokinetics of Fc-EDA1 used in patients, but also for diagnostic purpose. In Switzerland, at four days of life, all newborns undergo neonatal screening: a few drops of blood from the heel are dried on a sheet of blotting paper and analysed for seven hormonal and metabolic diseases. XLHED could be added on this screening if an efficient therapy can then be proposed.

The neonatal screening technic raises several difficulties. One the one hand, it uses only a few drops of dried blood. After elution from the paper, it should be tested whether enough serum can be collected to perform the ELISA. Furthermore, it should be tested whether high concentrations of haemoglobin would interfere with the ELISA. In addition, EDA could be denatured in blood dried on filter paper, with no guarantee that it would still be recognized in the ELISA. Nevertheless, all of these parameters could be relatively easily tested: recombinant EDA can be dried on filter paper, alone or in serum or in blood, then eluted and dosed by ELISA. If a signal is obtained, its specificity could be tested by pre-depletion of the eluted blood, as described in the result section, or by testing blood from an EDA-deficient patient.

All biochemical studies performed to date on EDA were done on recombinant or overexpressed EDA. The fact that EctoD2 can efficiently deplete EDA in serum suggests that it could be

used to affinity purify endogenous EDA from serum for the molecular characterization of endogenous EDA. A simple Western blot (using Renzo2 antibody) would indicate, for example, whether soluble EDA contains or not the collagen domain.

Finally, if the detection of EDA would be possible also in tissue extracts one could address interesting questions about the origin of EDA, and possibly how it is transported into the circulation.

# 7 Acknowledgment

I thank Pascal Schneider for giving me the opportunity to perform a master thesis in his laboratory and for his advice, suggestions and critics. Special thanks go to Christine Kowalczyk-Quintas, Sonia Schüpbach and Laure Willen for the good atmosphere in the lab, for their technical support and for their opinions. I am very grateful to the Mouse Pathology Facility, especially to Janine Horlbeck for advice and for the preparation of histology sections. I also want to thank Dr. Olivier Gaide for being the expert of my master thesis.

# 8 Bibliography

1. Mikkola ML, Thesleff I. Ectodysplasin signaling in development. Cytokine Growth Factor Rev. août 2003;14(3-4):211-24.
2. Itin PH. Etiology and pathogenesis of ectodermal dysplasias. Am J Med Genet A. 8 avr 2014;
3. Smahi A, Courtois G, Rabia SH, Döffinger R, Bodemer C, Munnich A, et al. The NF-kappaB signalling pathway in human diseases: from incontinentia pigmenti to ectodermal dysplasias and immune-deficiency syndromes. Hum Mol Genet. 1 oct 2002;11(20):2371-5.
4. Cluzeau C, Hadj-Rabia S, Jambou M, Mansour S, Guigue P, Masmoudi S, et al. Only four genes (EDA1, EDAR, EDARADD, and WNT10A) account for 90% of hypohidrotic/anhidrotic ectodermal dysplasia cases. Hum Mutat. janv 2011;32(1):70-2.
5. Mehta U, Brunworth J, Fete TJ, Sindwani R. Head and neck manifestations and quality of life of patients with ectodermal dysplasia. Otolaryngol-Head Neck Surg Off J Am Acad Otolaryngol-Head Neck Surg. mai 2007;136(5):843-7.
6. Wright JT, Grange DK, Richter MK. Hypohidrotic Ectodermal Dysplasia. In: Pagon RA, Adam MP, Ardinger HH, Bird TD, Dolan CR, Fong C-T, et al., éditeurs. GeneReviews (®) [Internet]. Seattle (WA): University of Washington, Seattle; 1993 [cité 11 juin 2014]. Disponible sur: http://www.ncbi.nlm.nih.gov/books/NBK1112/
7. Chassaing N, Bourthoumieu S, Cossee M, Calvas P, Vincent M-C. Mutations in EDAR account for one-quarter of non-ED1-related hypohidrotic ectodermal dysplasia. Hum Mutat. mars 2006;27(3):255-9.
8. Clarke A, Phillips DI, Brown R, Harper PS. Clinical aspects of X-linked hypohidrotic ectodermal dysplasia. Arch Dis Child. oct 1987;62(10):989-96.
9. Fete M, Hermann J, Behrens J, Huttner KM. X-linked hypohidrotic ectodermal dysplasia (XLHED): Clinical and diagnostic insights from an international patient registry. Am J Med Genet A. 24 mars 2014;

10. Tyagi P, Tyagi V, Hashim AA. Ocular and non-ocular manifestations of hypohidrotic ectodermal dysplasia. BMJ Case Rep. 2011;2011.
11. Hammersen JE, Neukam V, Nüsken K-D, Schneider H. Systematic evaluation of exertional hyperthermia in children and adolescents with hypohidrotic ectodermal dysplasia: an observational study. Pediatr Res. sept 2011;70(3):297-301.
12. Huttner K. Future developments in XLHED treatment approaches. Am J Med Genet A. 26 mars 2014;
13. Gaide O, Schneider P. Permanent correction of an inherited ectodermal dysplasia with recombinant EDA. Nat Med. mai 2003;9(5):614-8.
14. Casal ML, Lewis JR, Mauldin EA, Tardivel A, Ingold K, Favre M, et al. Significant correction of disease after postnatal administration of recombinant ectodysplasin A in canine X-linked ectodermal dysplasia. Am J Hum Genet. nov 2007;81(5):1050-6.
15. Bodmer J-L, Schneider P, Tschopp J. The molecular architecture of the TNF superfamily. Trends Biochem Sci. janv 2002;27(1):19-26.
16. Aggarwal BB. Signalling pathways of the TNF superfamily: a double-edged sword. Nat Rev Immunol. sept 2003;3(9):745-56.
17. Schneider P, Street SL, Gaide O, Hertig S, Tardivel A, Tschopp J, et al. Mutations leading to X-linked hypohidrotic ectodermal dysplasia affect three major functional domains in the tumor necrosis factor family member ectodysplasin-A. J Biol Chem. 1 juin 2001;276(22):18819-27.
18. Mikkola ML. TNF superfamily in skin appendage development. Cytokine Growth Factor Rev. août 2008;19(3-4):219-30.
19. Yan M, Wang LC, Hymowitz SG, Schilbach S, Lee J, Goddard A, et al. Two-amino acid molecular switch in an epithelial morphogen that regulates binding to two distinct receptors. Science. 20 oct 2000;290(5491):523-7.
20. Swee LK, Ingold-Salamin K, Tardivel A, Willen L, Gaide O, Favre M, et al. Biological activity of ectodysplasin A is conditioned by its collagen and heparan sulfate proteoglycan-binding domains. J Biol Chem. 2 oct 2009;284(40):27567-76.
21. Koppinen P, Pispa J, Laurikkala J, Thesleff I, Mikkola ML. Signaling and subcellular localization of the TNF receptor Edar. Exp Cell Res. 1 oct 2001;269(2):180-92.
22. Sun S-C. Non-canonical NF-$\kappa$B signaling pathway. Cell Res. 21 déc 2010;21(1):71-85.
23. Srivastava AK, Pispa J, Hartung AJ, Du Y, Ezer S, Jenks T, et al. The Tabby phenotype is caused by mutation in a mouse homologue of the EDA gene that reveals novel mouse and human exons and encodes a protein (ectodysplasin-A) with collagenous domains. Proc Natl Acad Sci U S A. 25 nov 1997;94(24):13069-74.
24. Ferguson BM, Brockdorff N, Formstone E, Ngyuen T, Kronmiller JE, Zonana J. Cloning of Tabby, the murine homolog of the human EDA gene: evidence for a membrane-associated protein with a short collagenous domain. Hum Mol Genet. sept 1997;6(9):1589-94.
25. Pispa J, Thesleff I. Mechanisms of ectodermal organogenesis. Dev Biol. 15 oct 2003;262(2):195-205.
26. Millar SE. Molecular mechanisms regulating hair follicle development. J Invest Dermatol. févr 2002;118(2):216-25.

27. Cui C-Y, Kunisada M, Esibizione D, Douglass EG, Schlessinger D. Analysis of the temporal requirement for eda in hair and sweat gland development. J Invest Dermatol. avr 2009;129(4):984-93.
28. Pummila M, Fliniaux I, Jaatinen R, James MJ, Laurikkala J, Schneider P, et al. Ectodysplasin has a dual role in ectodermal organogenesis: inhibition of Bmp activity and induction of Shh expression. Dev Camb Engl. janv 2007;134(1):117-25.
29. Jacob A, Chole RA. Survey Anatomy of the Paranasal Sinuses in the Normal Mouse. The Laryngoscope. 1 avr 2006;116(4):558-63.
30. Bojsen-Møller F. Topography of the nasal glands in rats and some other mammals. Anat Rec. 1 sept 1964;150(1):11-24.
31. Grüneberg H. The glandular aspects of the tabby syndrome in the mouse. J Embryol Exp Morphol. févr 1971;25(1):1-19.
32. Krstic RV. Human Microscopic Anatomy: An Atlas for Students of Medicine and Biology. Springer; 1991. 636 p.
33. Krstić RV. Die Gewebe des Menschen und der Säugetiere: ein Atlas zum Studium für Mediziner und Biologen. Springer; 1988. 426 p.
34. Taylor M. The origin and functions of nasal mucus. The Laryngoscope. avr 1974;84(4):612-36.
35. Kowalczyk-Quintas C, Willen L, Dang AT, Sarrasin H, Tardivel A, Hermes K, et al. Generation and characterization of function-blocking anti-ectodysplasin A (EDA) monoclonal antibodies that induce ectodermal dysplasia. J Biol Chem. 14 févr 2014;289(7):4273-85.
36. Kowalczyk C, Dunkel N, Willen L, Casal ML, Mauldin EA, Gaide O, et al. Molecular and Therapeutic Characterization of Anti-ectodysplasin A Receptor (EDAR) Agonist Monoclonal Antibodies. J Biol Chem. 5 juill 2011;286(35):30769-79.
37. Kowalczyk-Quintas C, Schuepbach-Mallepell S, Willen L, Smith TK, Huttner K, Kirby N, et al. Pharmacological Stimulation of Edar Signaling in the Adult Enhances Sebaceous Gland Size and Function. J Invest Dermatol. 10 sept 2014;
38. Broman I. Über die Entwickelung der konstanten grösseren Nasenhöhlendrüsen der Nagetiere.
39. Gruneberg H. The Tabby Syndrome in the Mouse. Proc R Soc Lond B Biol Sci. 16 nov 1971;179(1055):139-56.
40. Kowalczyk-Quintas C, Schneider P. Ectodysplasin A (EDA) - EDA receptor signalling and its pharmacological modulation. Cytokine Growth Factor Rev. avr 2014;25(2):195-203.
41. Hermes K, Schneider P, Krieg P, Dang A, Huttner K, Schneider H. Prenatal Therapy in Developmental Disorders: Drug Targeting via Intra-Amniotic Injection to Treat X-Linked Hypohidrotic Ectodermal Dysplasia. J Invest Dermatol. 20 juin 2014;
42. Cui C-Y, Durmowicz M, Ottolenghi C, Hashimoto T, Griggs B, Srivastava AK, et al. Inducible mEDA-A1 transgene mediates sebaceous gland hyperplasia and differential formation of two types of mouse hair follicles. Hum Mol Genet. 15 nov 2003;12(22):2931-40.